“Molecules in Intense Laser Fields – Femto to Atto to ZeptoSecond Dynamics”

and / or

“FAZSST-Femto-Atto-ZeptoSecond Science & Technology”

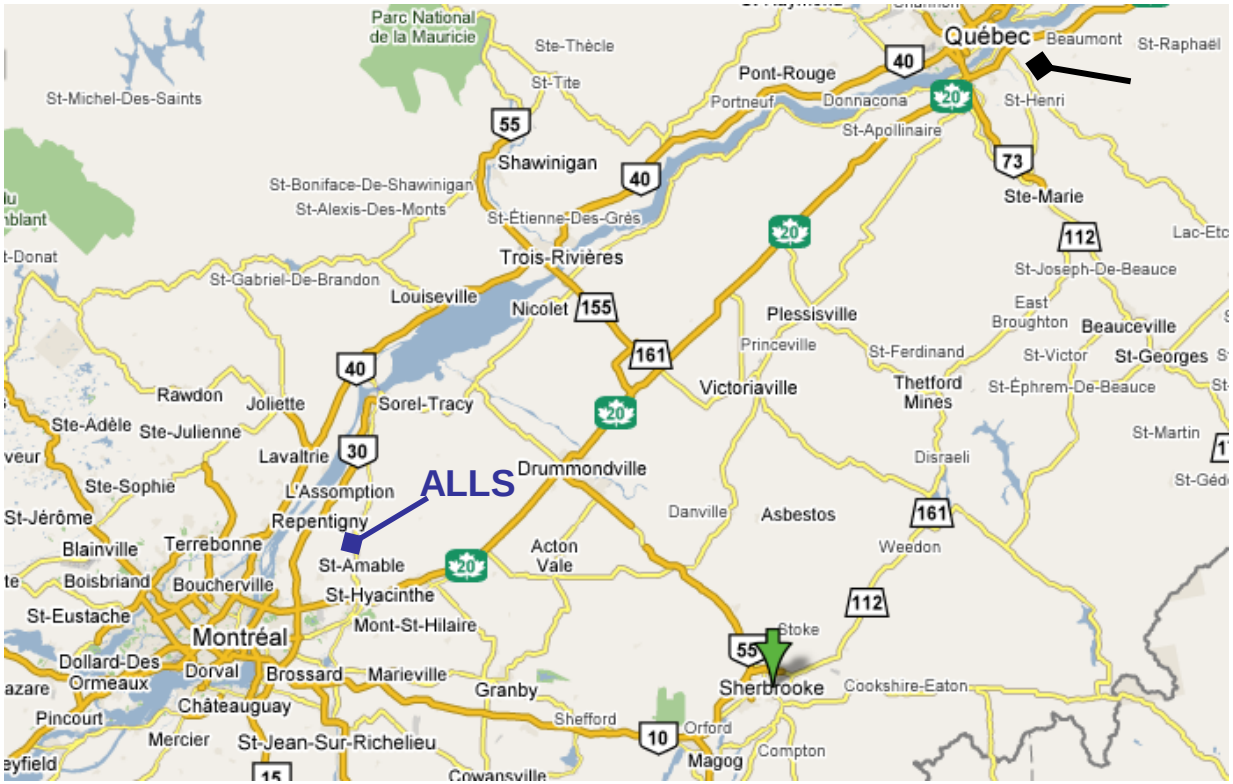

André D, Bandrauk, PhD, FRSC, FAAAS ,O C

Canada Research Chair

Computational Chemistry & Molecular Photonics

Université de Sherbrooke

Potential energy : $V_o : \frac{e^2}{a_0} = 1 \; Hartree = 27.2 \; eV,$ (1)

Electric field $\mathbf{E}_o : \frac{e}{a_o^2} = 5 \times 10^9 \; V/cm,$ (2)

Intensity $I_0 = cE_0^2/8\pi = 3.5 \times 10^{16} \, W/cm^2,$ (3)

Distance $a_0 = 0.0529 nm,$ (4)

Time : $t(a_0)$=24 as, $2\pi t_0$=152 as
$t(mc^2)$=1.3 zeptos

Table I

Evolution of Laser Parameters [1]

Time (s)		Intensity (Watts/cm^2)		Year
Nano	10^{-9}	Giga	10^{+9}	1980
Pico	10^{-12}	Tera	10^{+12}	1985
SERS				
Femto	10^{-15}	Peta	10^{+15}	1990
1a.u : 24 x 10^{-18}		$I_0 = 3.5 \times 10^{+16}$		
Atto	10^{-18}	Exa	10^{+18}	2005
Zepto	10^{-21}	Zetta	10^{+21}	2009
Yocto	10^{-24}	Yotta	10^{+24}	?

10^{29} - **Schwinger Limit**

The intensities discussed in the present article, $10^{14} \geq I \geq 10^{15} W/cm^2$ correspond to fields approaching the internal Coulomb potentials of atoms and molecules (V_0, equations (1-3), thus inducing considerable distortions of intermolecular potentials. In the dressed state representation these radiatively induced distortions creating LIMP's as discussed above lead to *bond softening* via laser-induced avoided crossing of molecular potentials [26-27]. At such intensities, one needs to consider further ionization and the remaining molecular ion potentials become LIMP's in the presence of intense laser pulses. The molecular ions, bound or dissociative can also undergo Above Threshold Dissociation, ATD, [20], [26-27],

Schwinger limit ~ 10**29 W/cm2)

Sunlight: 0.12 W/cm2

structure and dynamics in the microcosm

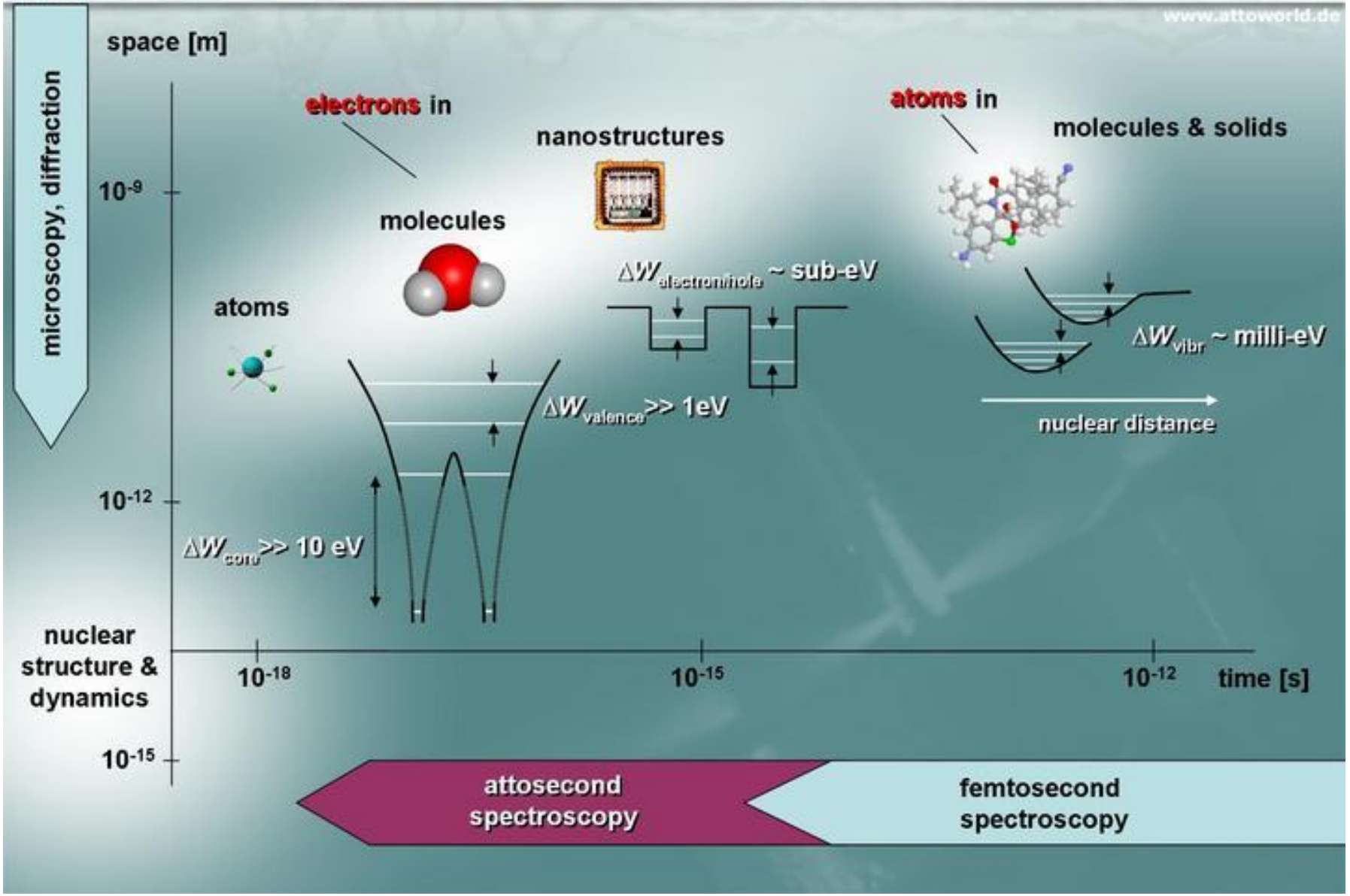

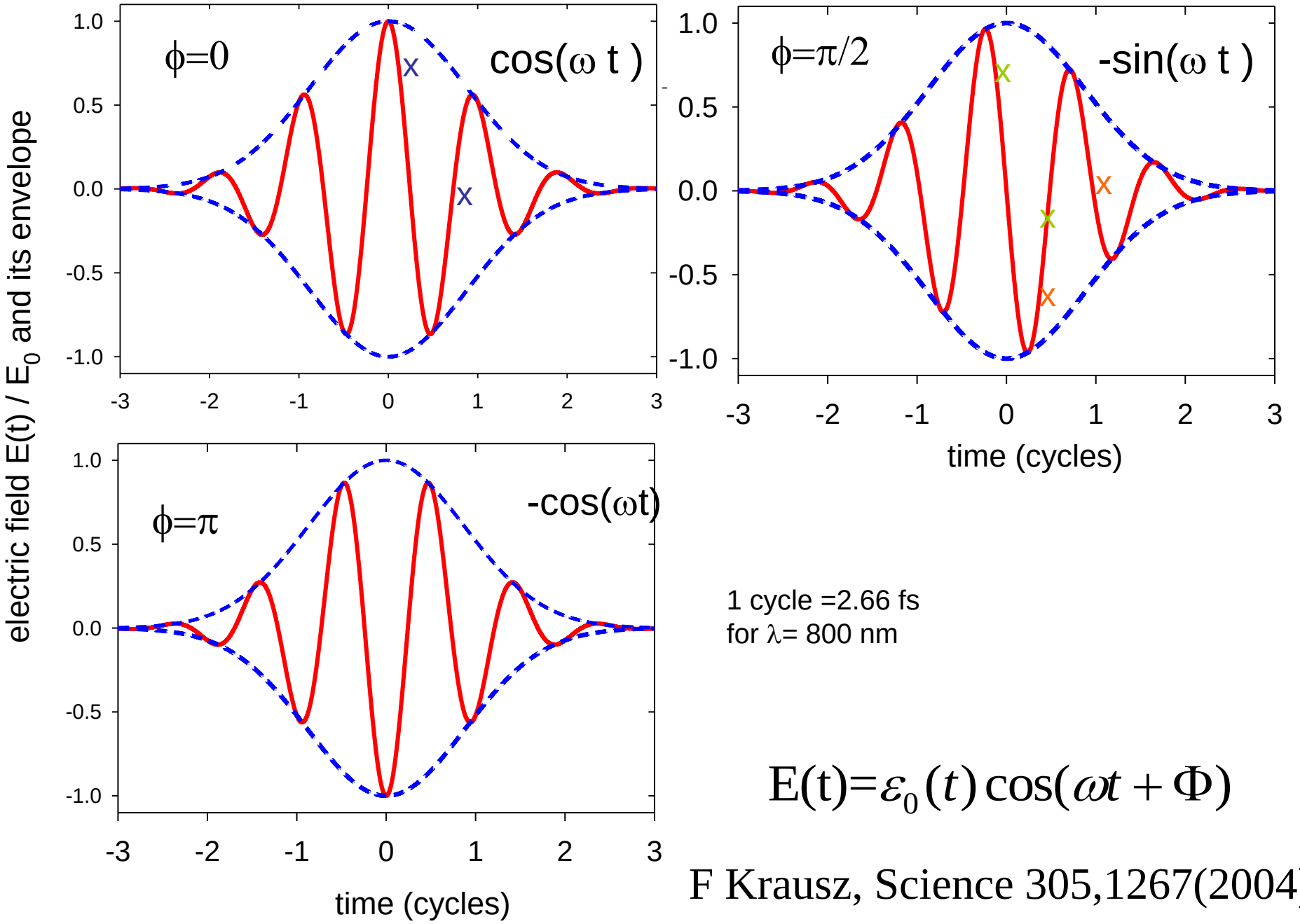

1 cycle =2.66 fs
for λ= 800 nm

$$E(t)=\varepsilon_0(t)\cos(\omega t+\Phi)$$

F Krausz, Science 305,1267(2004)

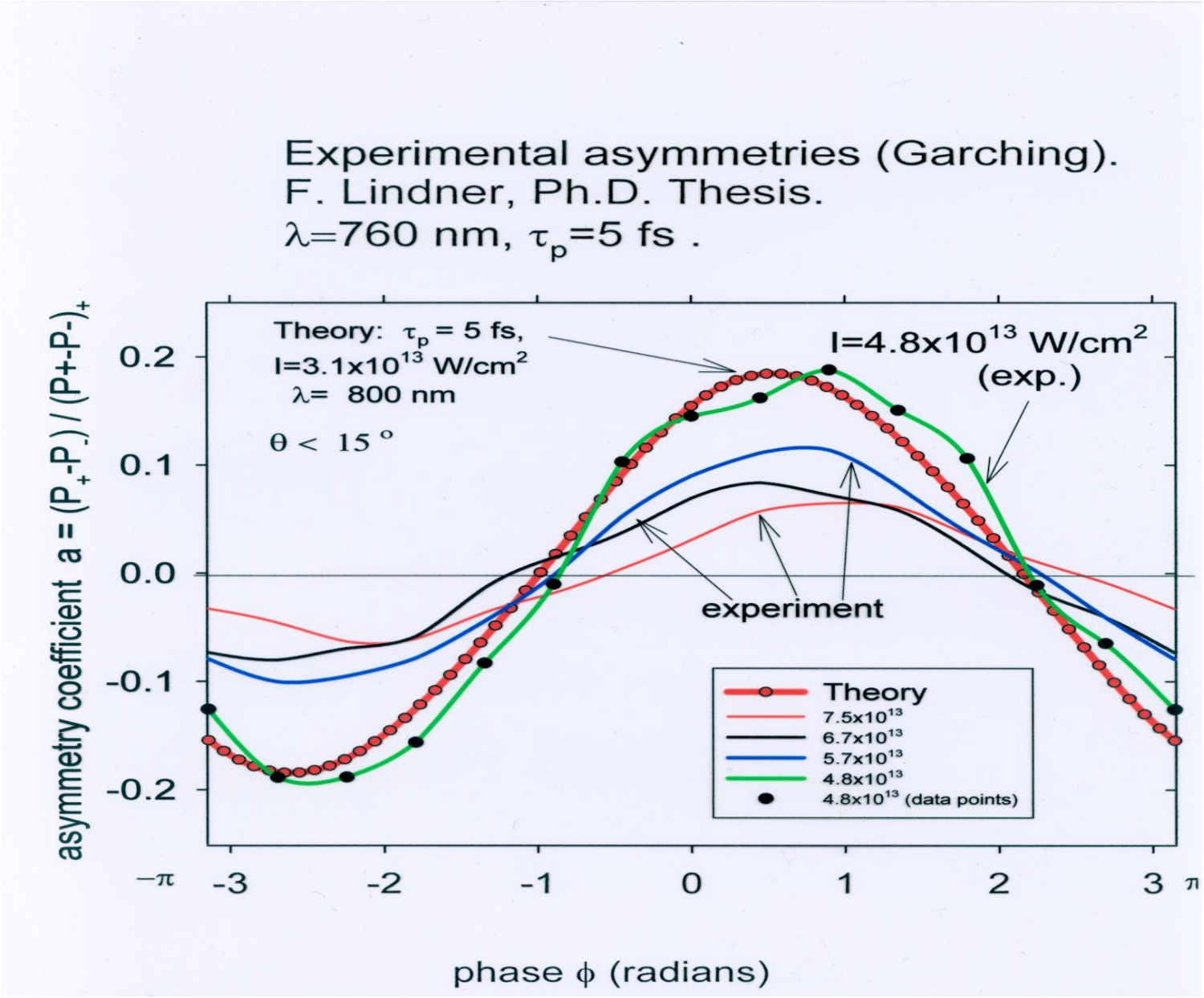

- **Phys. Rev. A, 70, 013815 (2004)**
- **Opt. Lett. 29, 1557 (2004)**

MAXWELL – SCHROEDINGER

Classical **Quantum**

MAXWELL

$$\frac{\partial^2 E}{\partial z^2} - \frac{1}{c^2}\frac{\partial^2 E}{\partial t^2} = \frac{4\pi}{c^2}\frac{\partial^2 P}{\partial t^2}$$

P = Medium Polarization = P(E)

(1^{st} Order P = αE)

SCHROEDINGER

$$i\hbar\frac{\partial|\psi\rangle}{\partial t} = \left(\hat{H}_0 + \hat{V}(t)\right)|\psi\rangle$$

$$P = P(E) = n_0\langle\psi|\hat{\mu}_0|\psi\rangle$$

$$|\psi\rangle = \sum_j c_j e^{iE_j t/\hbar}|\Psi_j\rangle$$

$$V_{ii} = -P_{ii}\left(e(z,t)\cos(kz-\omega t)\right)$$

$$N_p = \underbrace{10^3}_{z_1} \times \underbrace{10^3}_{z_2} \times \underbrace{10^2}_{\delta_1} \times \underbrace{10^2}_{\delta_2} \times \underbrace{10^2}_{\phi} \simeq 10^{12} \times \underbrace{10^z}_{p} \simeq 10^{14}$$

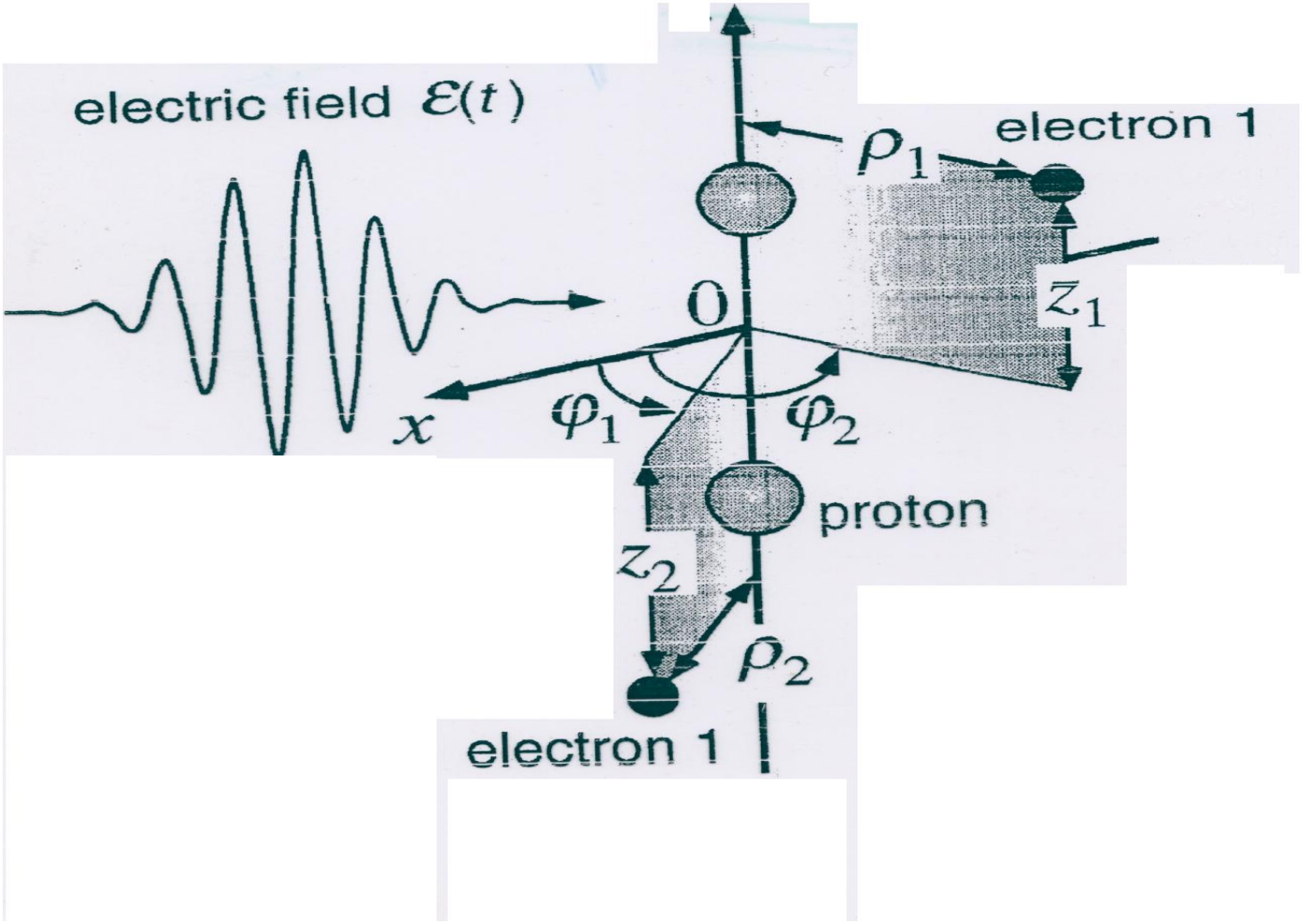

Phys. Rev. A **66**, 043403 (2002)

H_2 ($X^1\Sigma_g^+$): I=3x10^{15}W/cm^2, λ=800nm, T = 6 cycles

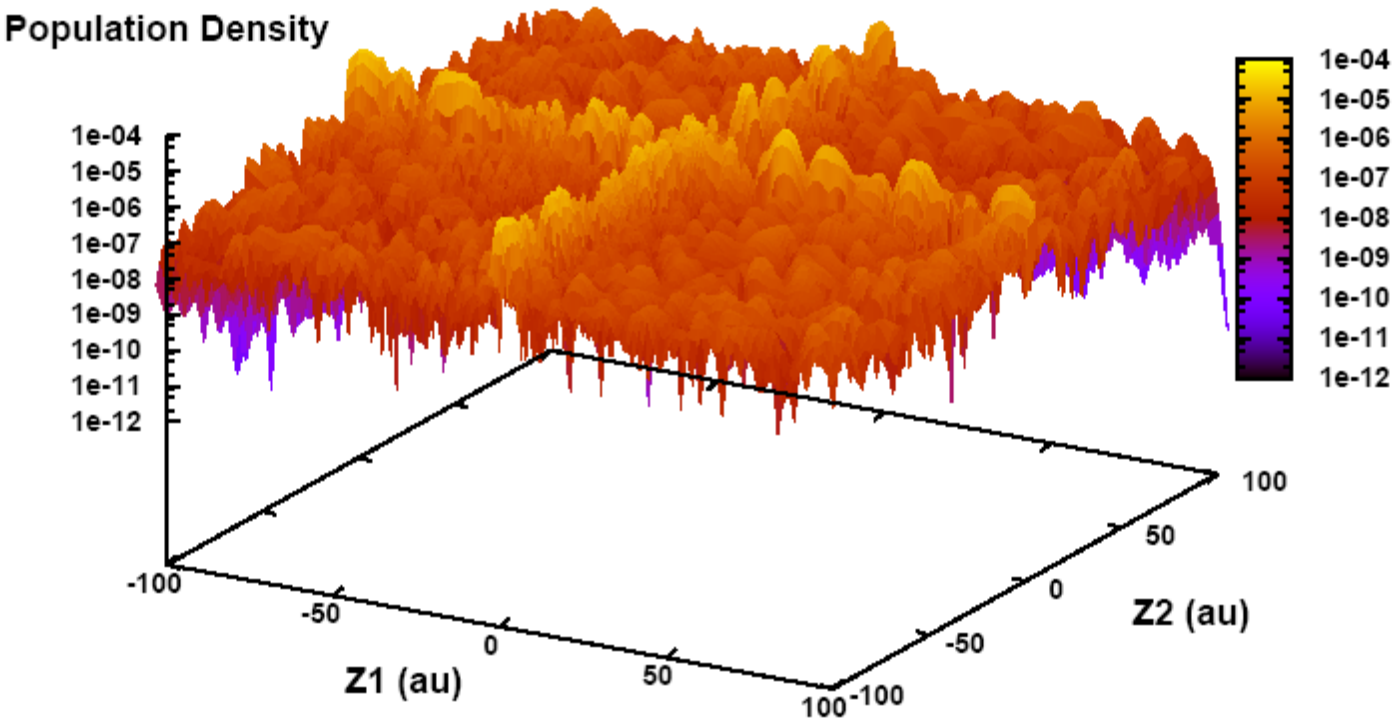

Available online at www.sciencedirect.com
SCIENCE DIRECT®
Chemical Physics Letters 419 (2006) 346–350
CHEMICAL PHYSICS LETTERS
www.elsevier.com/locate/cplett

Complex integration steps in decomposition of quantum exponential evolution operators

André D. Bandrauk [1], Effat Dehghanian *, Huizhong Lu

Laboratoire de Chimie Théorique, Faculté des Sciences, Université de Sherbrooke, Qué., Canada J1K 2R1

Received 28 October 2005; in final form 1 December 2005
Available online 22 December 2005

Abstract

We generalize previous high-order exponential split operator methods for solving time-dependent Schroedinger equations [A.D. Bandrauk, H. Shen, Chem. Phys. Lett. 176 (1991) 428] by introducing complex integration steps ($a + ib$) with real positive part a. We show that this new procedure avoids real negative steps which occur generally in high-order split operator methods. New highly accurate splitting schemes are thus derived and the efficiency of these is demonstrated in the calculation of the eigenstates of the one-electron molecular ion H_2^+.

We enumerate the pairs of integrators with second, third and fourth-order accuracies for later numerical comparison:

$$S_2^A = e^{\gamma\lambda A} e^{\lambda B} e^{\gamma^*\lambda A} + (O(\lambda^3)), \quad \gamma = \frac{1}{2}, \tag{18}$$

$$S_2^B = e^{\gamma\lambda B} e^{\lambda A} e^{\gamma^*\lambda B} + (O(\lambda^3)), \quad \gamma = \frac{1}{2}, \tag{19}$$

$$S_3^B = e^{\gamma\lambda B/2} e^{\gamma\lambda A} e^{\lambda B/2} e^{\gamma^*\lambda A} e^{\gamma^*\lambda B/2} + (O(\lambda^4)),$$
$$\gamma = \frac{1}{2}\left(1 \pm \frac{i}{\sqrt{3}}\right), \tag{20}$$

$$S_3' = \frac{1}{2}(e^{\gamma\lambda B} e^{\lambda A} e^{\gamma^*\lambda B} + e^{\gamma\lambda A} e^{\lambda B} e^{\gamma^*\lambda A}) + (O(\lambda^4)),$$
$$\gamma = \frac{1}{2}\left(1 \pm \frac{i}{\sqrt{3}}\right), \tag{21}$$

$$S_4^B = e^{\gamma\lambda B/2} e^{\gamma\lambda A} e^{(1-\gamma)\lambda B/2} e^{(1-2\gamma)\lambda A} e^{(1-\gamma)\lambda B/2} e^{\gamma\lambda A} e^{\gamma\lambda B/2}$$
$$+ (O(\lambda^5)), \quad \gamma = (2 - 2^{1/3})^{-1}, \tag{22}$$

$$S_4' = \frac{1}{2}(e^{\gamma\lambda B/2} e^{\lambda A/2} e^{\gamma^*\lambda B} e^{\lambda A/2} e^{\gamma\lambda B/2} + e^{\gamma\lambda A/2} e^{\lambda B/2} e^{\gamma^*\lambda A} e^{\lambda B/2} e^{\gamma\lambda A/2})$$
$$+ (O(\lambda^5)), \quad \gamma = \frac{1}{2} \pm \frac{i}{2\sqrt{3}}. \tag{23}$$

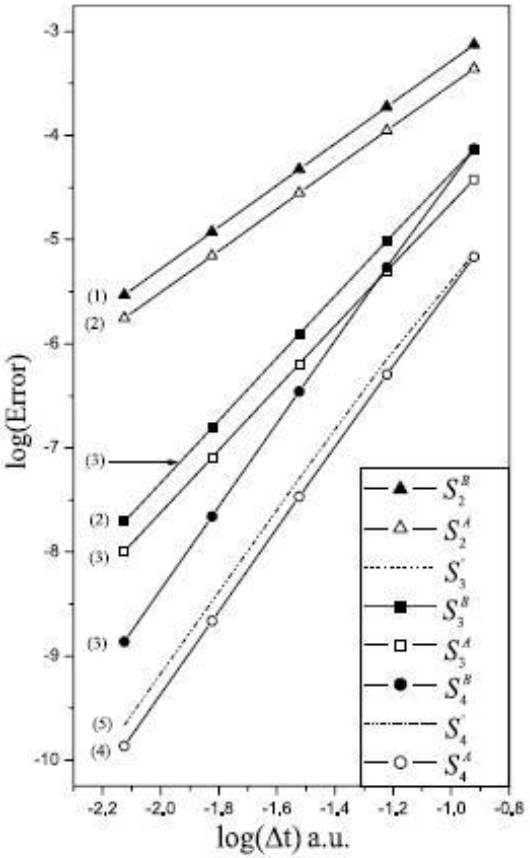

Fig. 1. Test of convergence for ground state of H_2^+ (Eqs. 25 and 26). *m* corresponds to number of FFT's, N_{FFT}.

Top 25 Hottest Articles

ScienceDirect Top 25 Articles Overall

October - December 2007

RSS

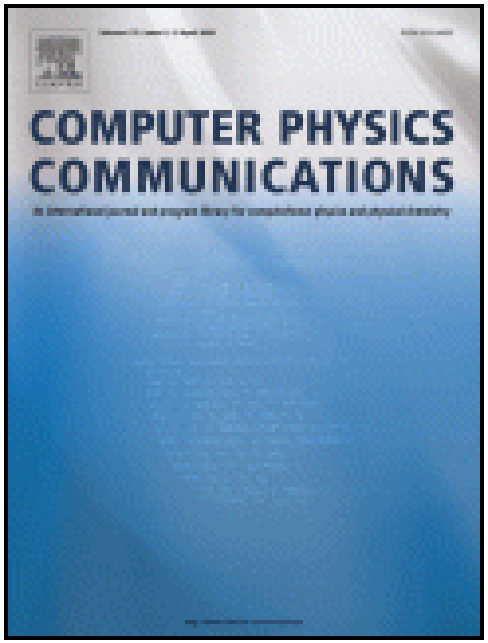

A numerical Maxwell–Schrödinger model for intense laser–matter interaction and propagation

E. Lorin[a, b, ,] , S. Chelkowski[c] and A. Bandrauk[d]

[a]Centre de Recherche en Mathématiques de Montréal, University of Montréal, Canada

Applied maths,[,]Carleton [d],University,Ottawa ,

Laboratoire de Chimie Theorique,U de Sherbrooke

Model

Coupling of macroscopic Maxwell's equations with many TDSE's.

Lorin, Chelkowski, Bandrauk, Comput. Phys. Comm. vol. 177 (2007)

$$
\begin{cases}
\partial_t \mathbf{B}(\mathbf{r},t) &= -\nabla \times \mathbf{E}(\mathbf{r},t) \\
\partial_t \mathbf{E}(\mathbf{r},t) &= \nabla \times \mathbf{B}(\mathbf{r},t) - 4\pi \partial_t \mathbf{P}(\mathbf{r},t) \\
\nabla \cdot \mathbf{B}(\mathbf{r},t) &= 0 \\
\nabla \cdot \big(\mathbf{E}(\mathbf{r},t) + \mathbf{P}(\mathbf{r},t)\big) &= 0 \\
\\
\mathbf{P}(\mathbf{r},t) = n(\mathbf{r}) \sum_{i=1}^{m} \mathbf{P}_i(\mathbf{r},t) &= n(\mathbf{r}) \sum_{i=1}^{m} \chi_{\Omega_i}(\mathbf{r}) \int_{\mathbb{R}^3} \psi_i \mathbf{r}' \psi_i^* \\
\mathtt{i}\partial_t \psi_i(\mathbf{r}',t) &= -\frac{\triangle_{\mathbf{r}'}}{2}\psi_i + \mathbf{r}' \cdot \mathbf{E}_{\mathbf{r}_i}\psi_i + V_c \psi_i, \\
& \qquad \forall i \in \{1,\ldots,m\}
\end{cases}
$$

The numerical model is the one presented in [19], where the gas domain is divided in small cells of gas denoted by Δv (corresponding the Ω_i's of Section 2) and in which we solve 1 TDSE, representing the $n\Delta v$ molecules of the cell. In practice 3d Maxwell's equations are solved in parallel with $\sim 140,000$ 1d TDSE's, see Fig. 5 and [17]. We then represent at

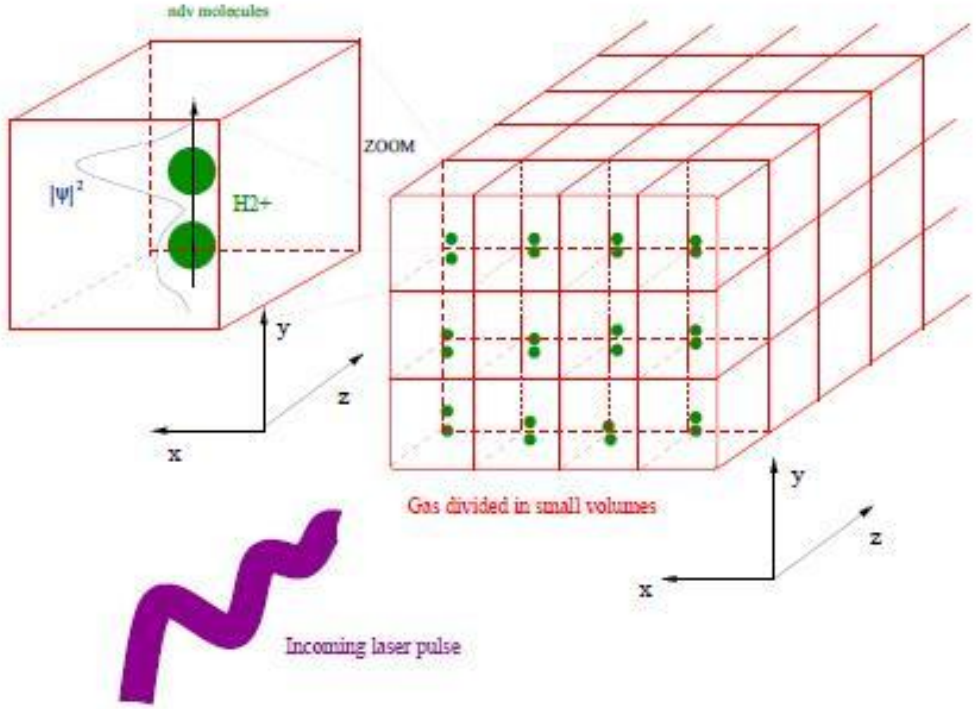

Figure 5: Numerical geometry

Improvement of the model I - microscopic approach

Another approach is presented in Lorin, Bandrauk, Chelkowski, Num. Methods for Partial Diff. Eq., (2008). A method to transmit free electron from a molecule to another. Based on a particular choice of boundary conditions (Volkov)

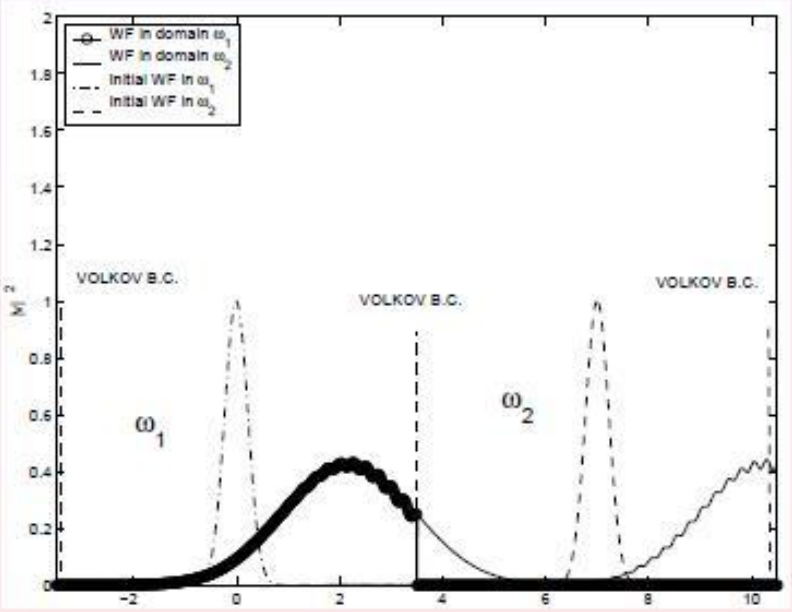

Figure: Free electron transmission

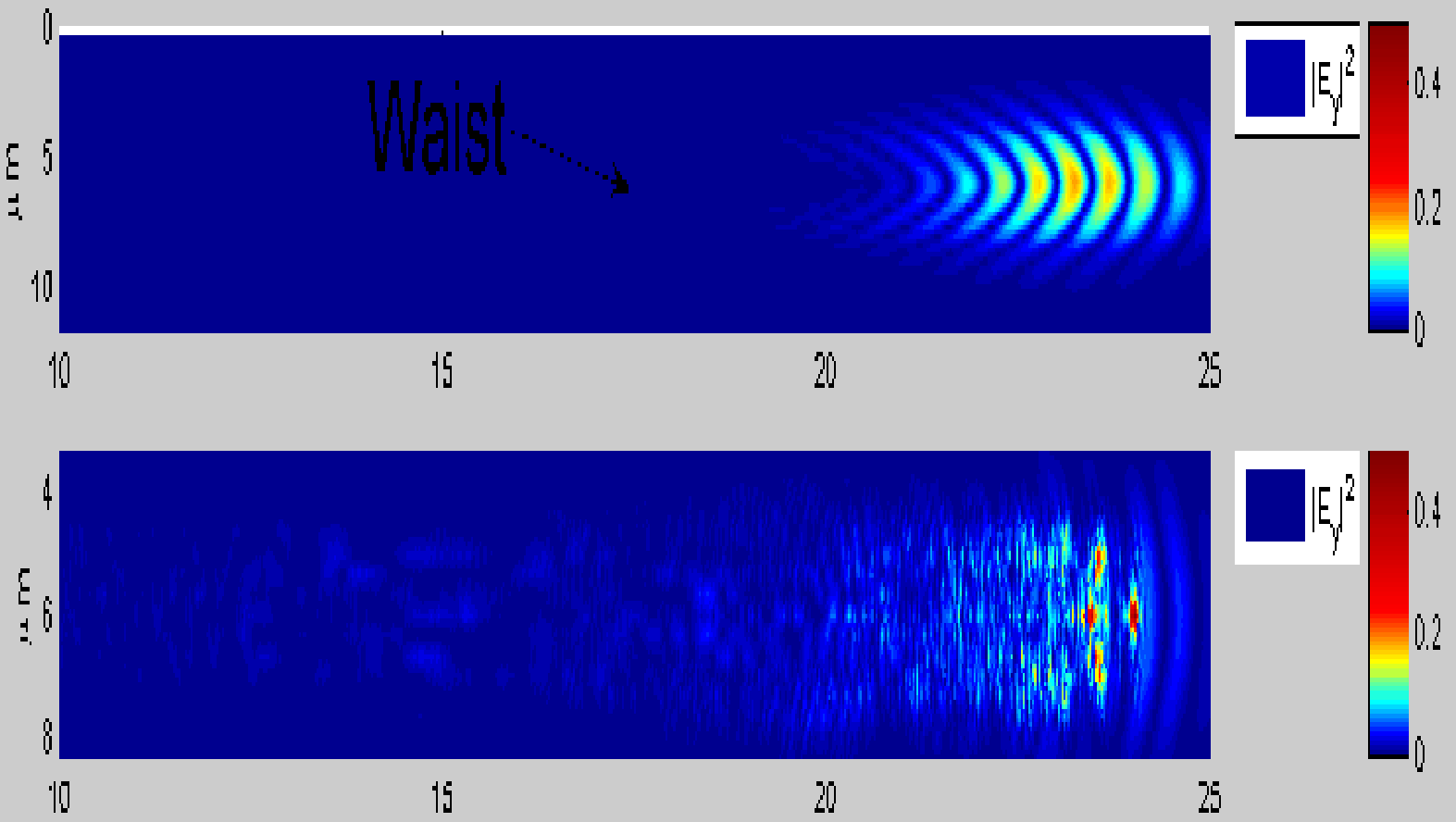

New J Phys 10,025033(2008)

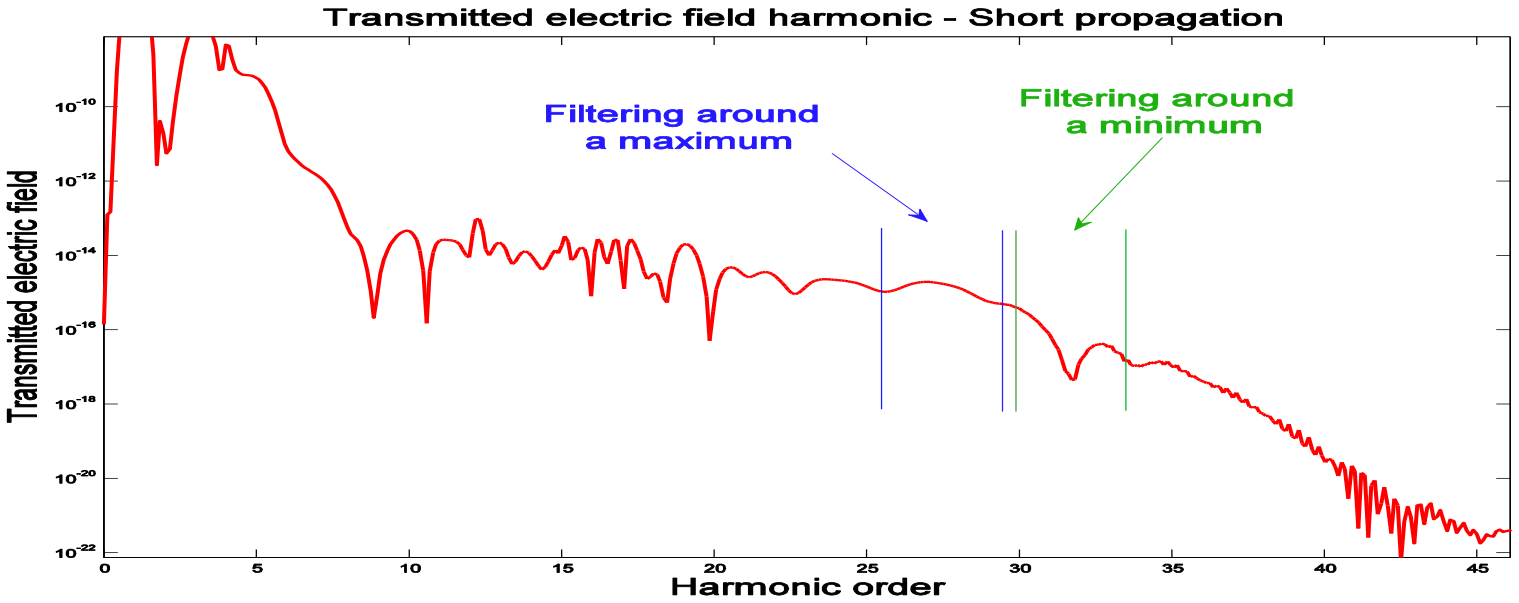

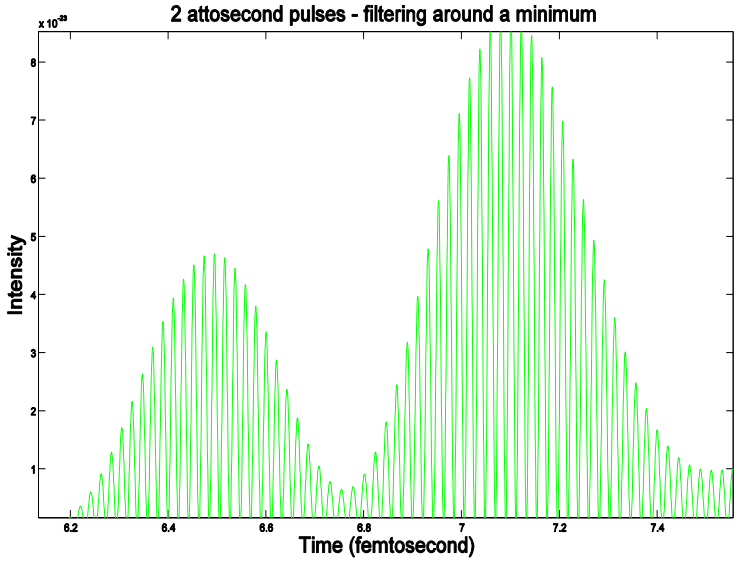

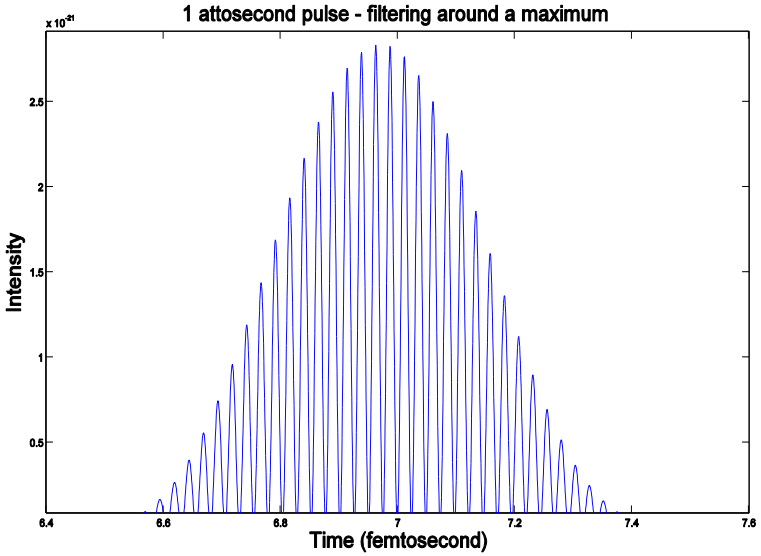

Two (minimum) or one (maximum) attosecond pulses

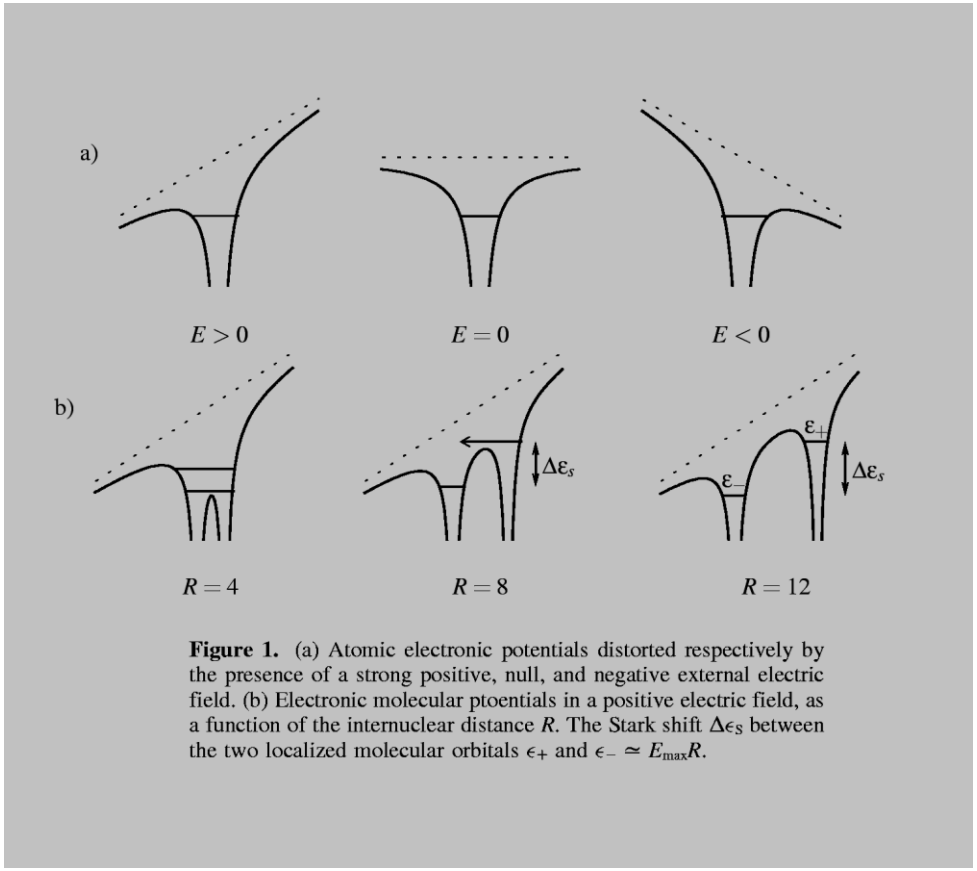

Figure 1. (a) Atomic electronic potentials distorted respectively by the presence of a strong positive, null, and negative external electric field. (b) Electronic molecular ptoentials in a positive electric field, as a function of the internuclear distance R. The Stark shift $\Delta\epsilon_S$ between the two localized molecular orbitals ϵ_+ and $\epsilon_- \simeq E_{max}R$.

P. B. Corkum, PRL, 71, 1994 (1993).

T. Zuo and A. D. Bandrauk, PRA, 52, R2511 (1995).

Charge Resonance Enhanced Ionization

CREI

Field ionization model

A^+ --- e^- --- A^+

$E(t_0)<0$

$Rc = 4 / I_p$

$E(t_2)>0$

$E(t_1)=0$

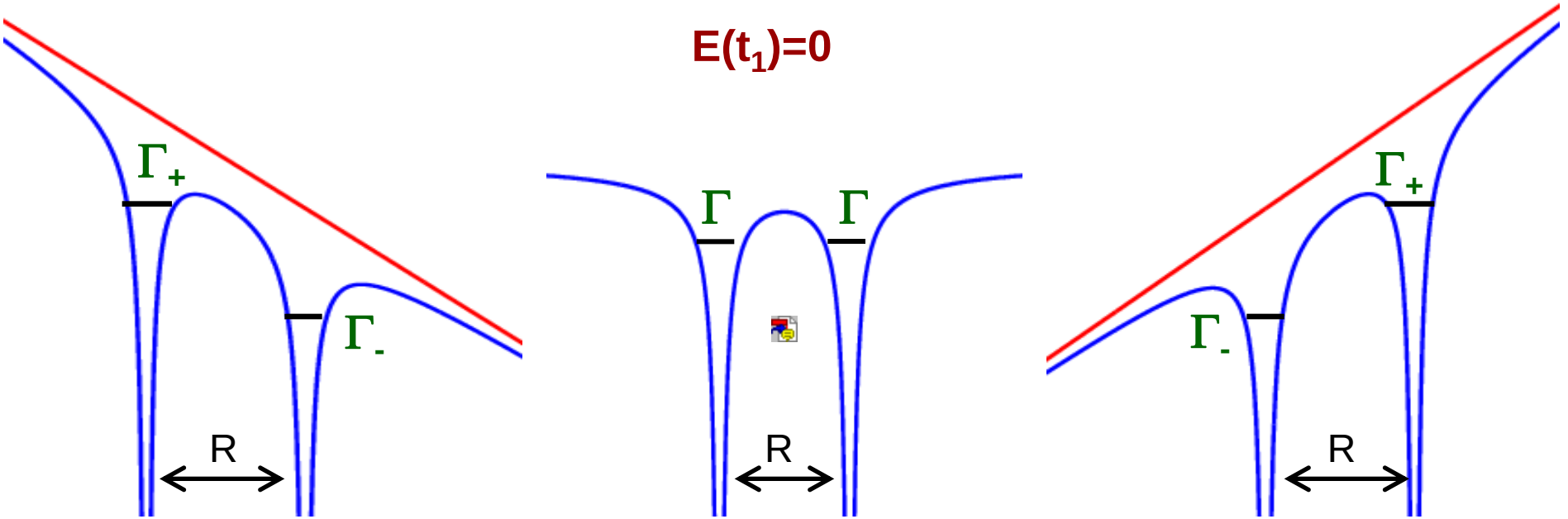

Localization + Ionization

$\Gamma_+ > \Gamma_-$

$E_+ \approx E(t_0) + E_c(R)$

$E_- \approx E(t_0) - E_c(R)$

delocalization via Tunnelling

(Γ, ω_L)

Localization + Ionization

$\Gamma_+ > \Gamma_-$

$E_+ \approx E(t_2) + E_c(R)$

$E_- \approx E(t_2) - E_c(R)$

T. Zuo and A.D.B., Phys. Rev. A **57**, 2511 (1995) ==> **3D**

T. Seideman et al, Phys. Rev. lett. **75**, 2819 (1995) ==> **1D**

S. Chelkowski and A,D,B., J. Phys. B **28**, L723 (1995) ==> **1D**

Schroeder, Uiterwaal, Kompa, Las. Phys. 10, 749 (2000). ==> **3D**

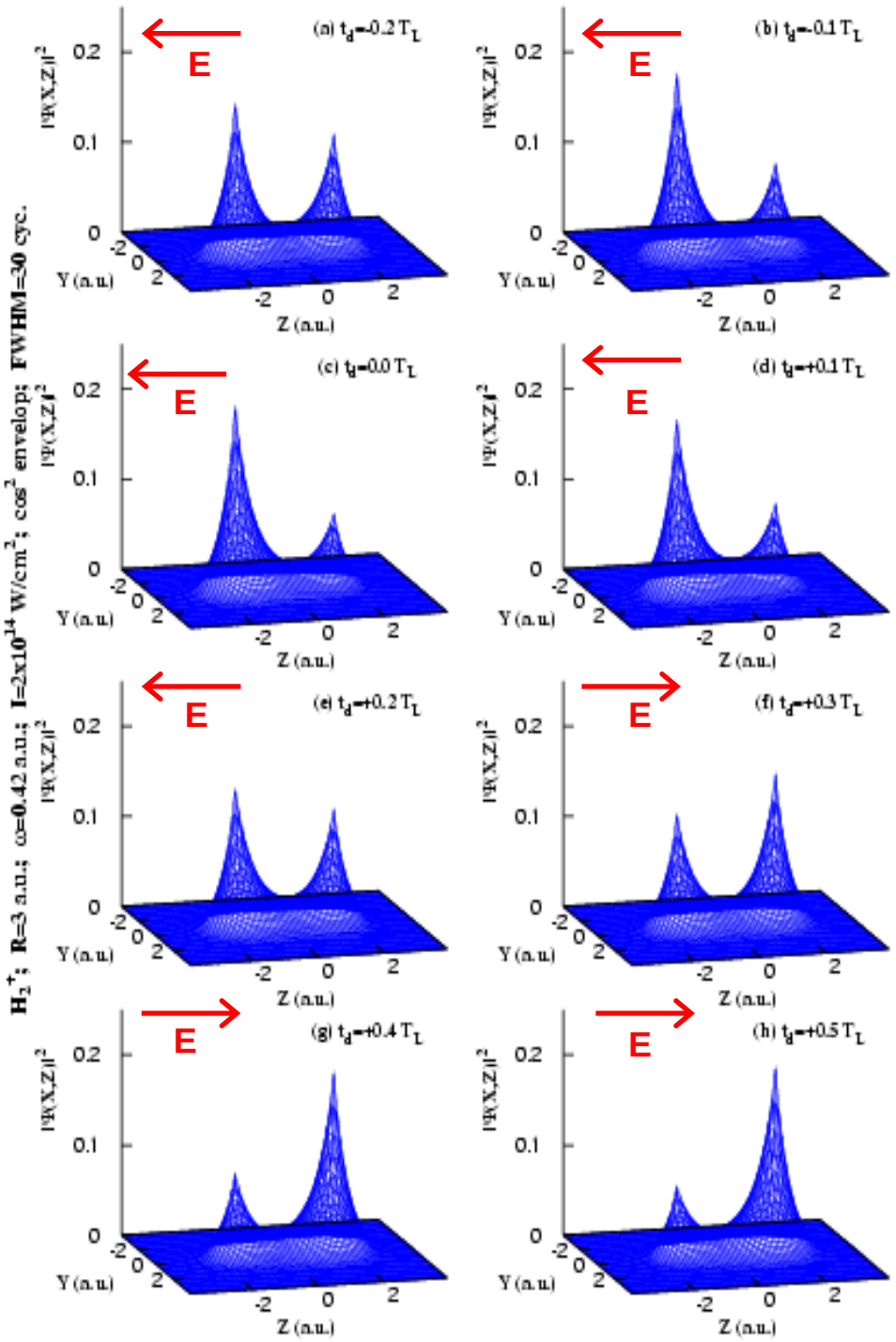

Non-adiabatic: electron does not follow the field E

H_2^+:
R=3 a.u.
w=0.42 a.u.
I=2x10^{14} W/cm^2

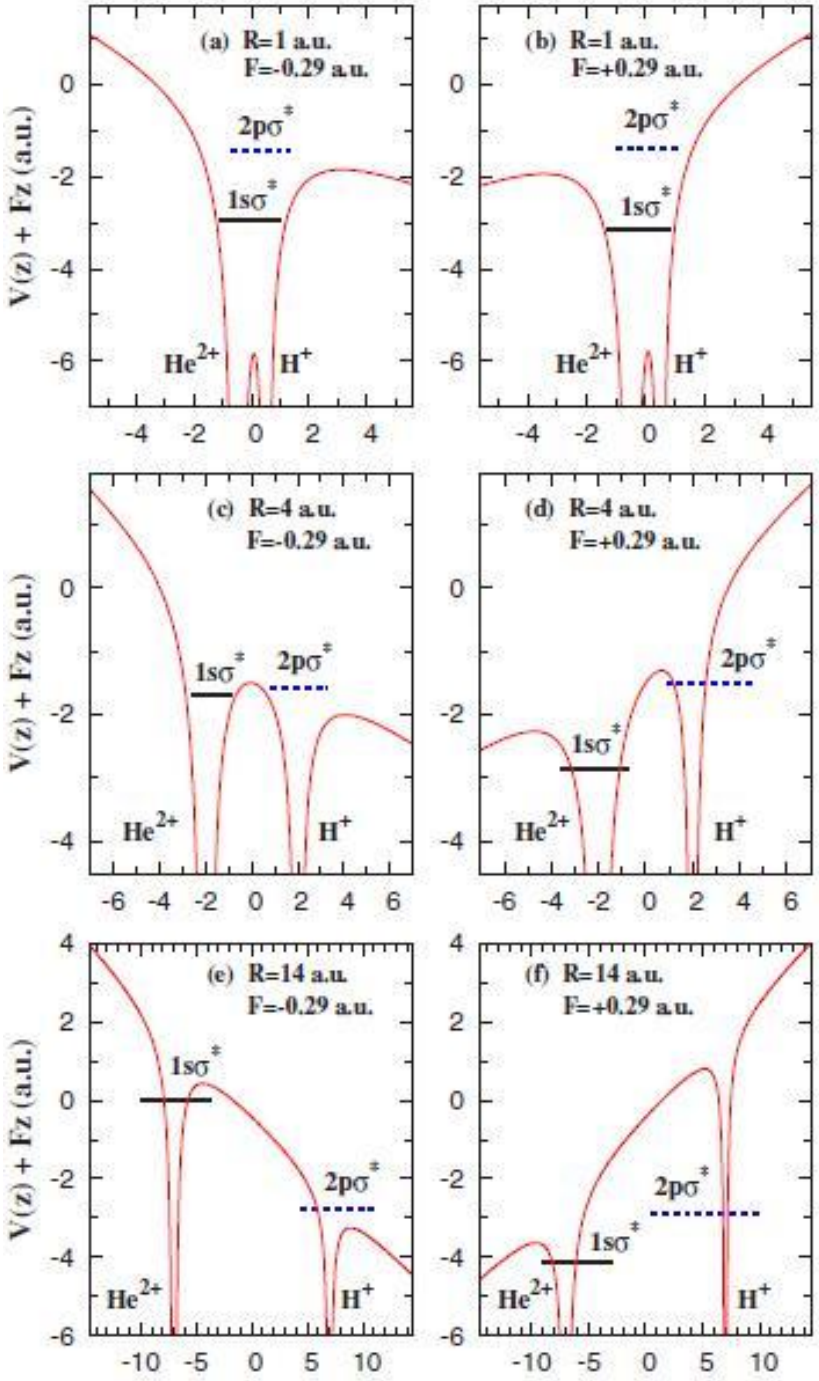
(a) R=1 a.u.
F=-0.29 a.u.
(b) R=1 a.u.
F=+0.29 a.u.
(c) R=4 a.u.
F=-0.29 a.u.
(d) R=4 a.u.
F=+0.29 a.u.
(e) R=14 a.u.
F=-0.29 a.u.
(f) R=14 a.u.
F=+0.29 a.u.
V(z) + Fz (a.u.)
2pσ*
1sσ*
He2+
H+

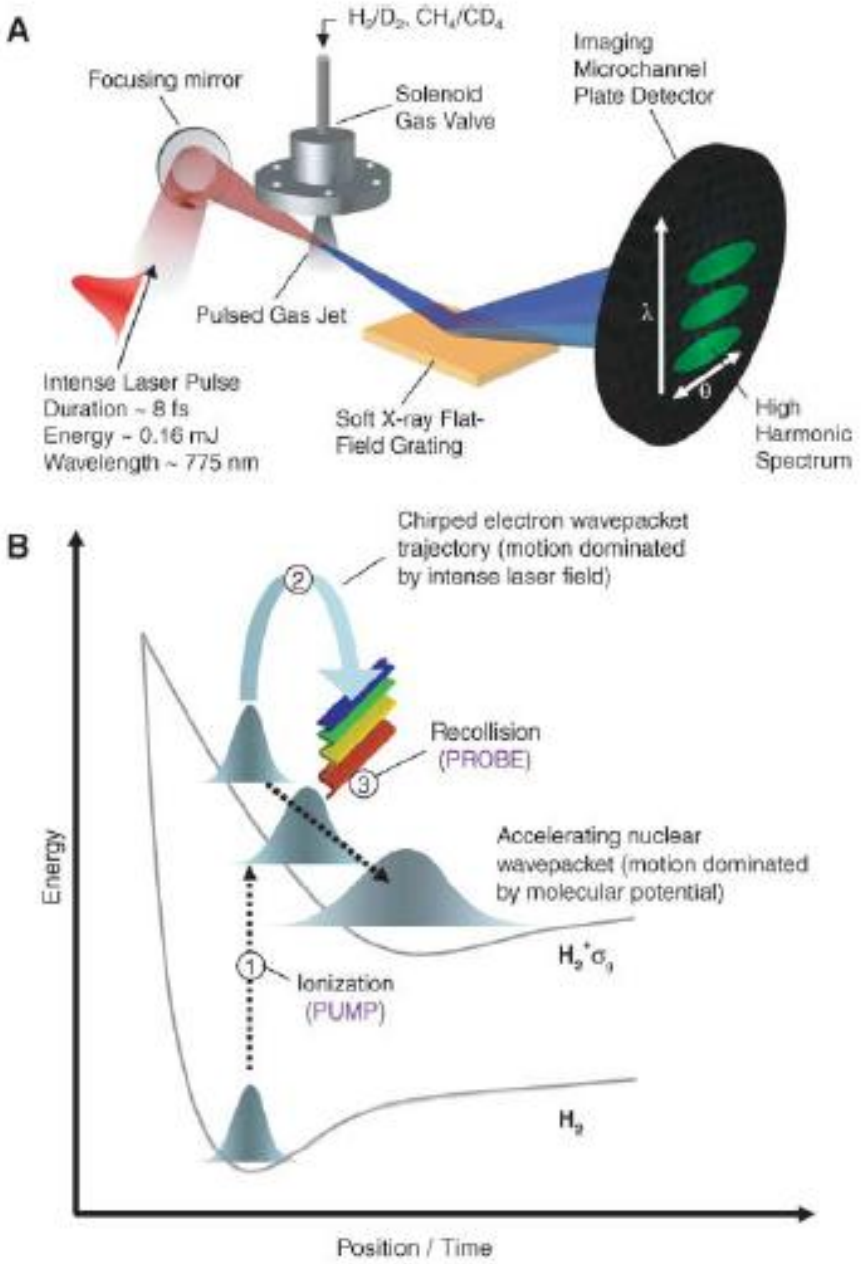

Corkum (Legare) – Bandrauk, Nature 417, 917 (2002)

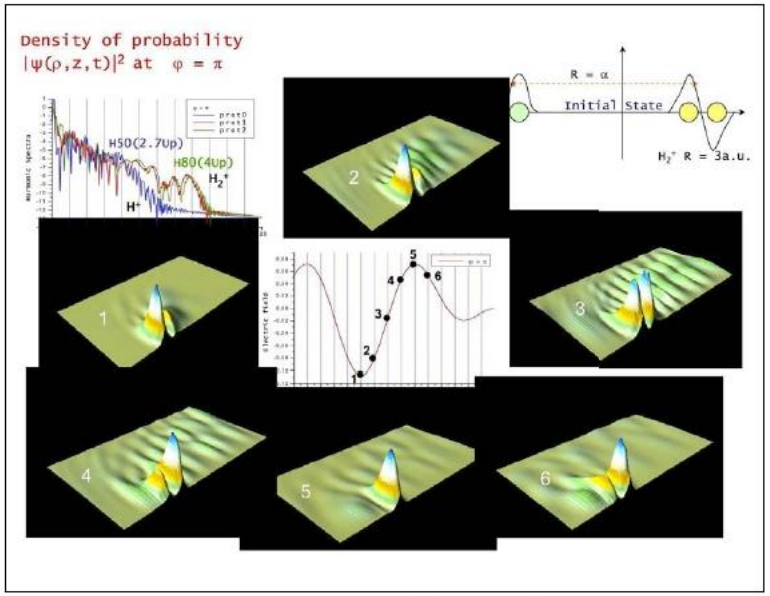

Le sytème moléculaire H^+ (gauche) + H_2^+ (droite) en présence d'un champ (électrique) laser

On voit la distribution ondulatoire de l'électron se déplacer de gauche à droite selon l'intensité du champ (dont les valeurs sont données par les points de 1 à 6). Une partie de l'électron se dissipe comme des ondes d'eau à cause de l'ionisation.

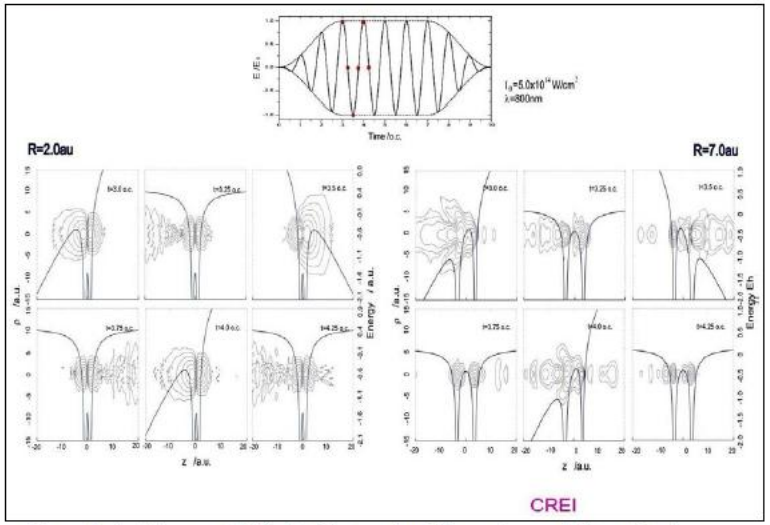

Exemple de déplacement de l'onde d'électron dans H_2^+ en présence de l'impulsion laser (à des distances internucléaires différentes)

On voit l'électron suivre plus ou moins le champ électrique (représenté par un point rouge), ce qui permet d'envisager le contrôle du mouvement d'un électron dans une molécule par laser en dépit de la nature ondulatoire de l'électron.

ADB,S.Barmaki,GKamta

PhysRevLett 98,013001 (2007)

KJ Yuan,ADB
PRA 80,053404 (2009)

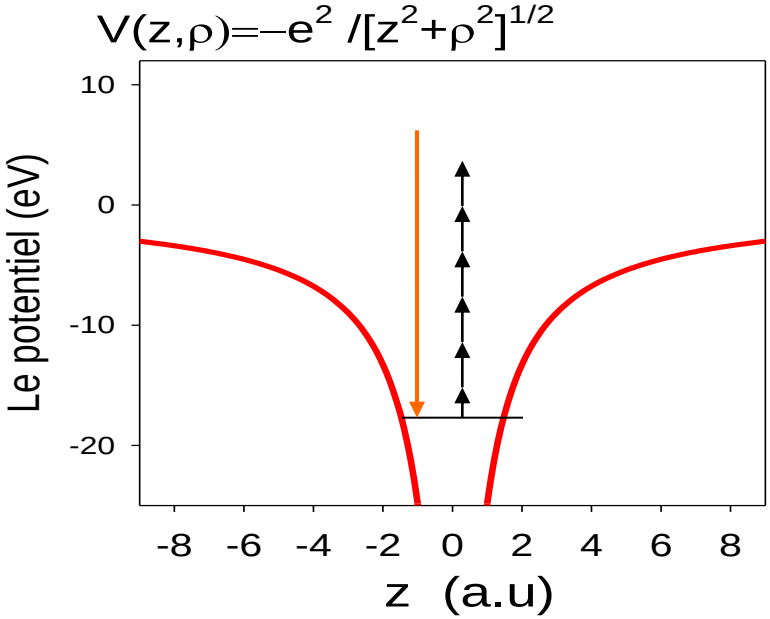

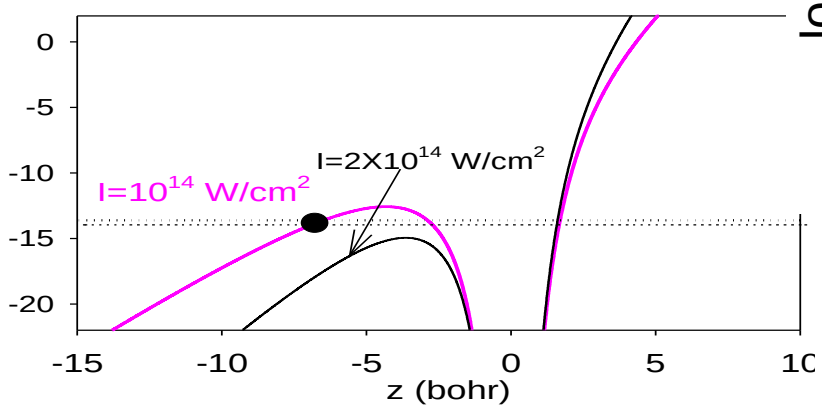

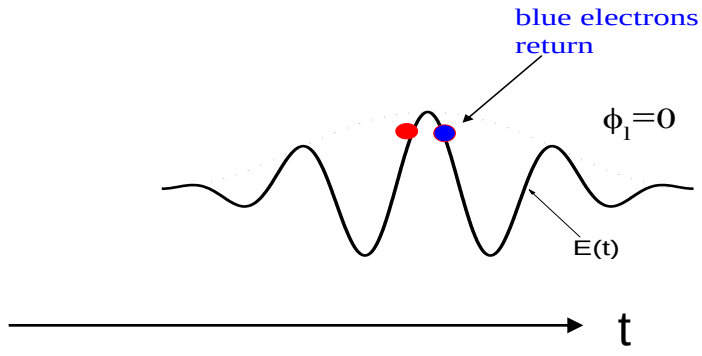

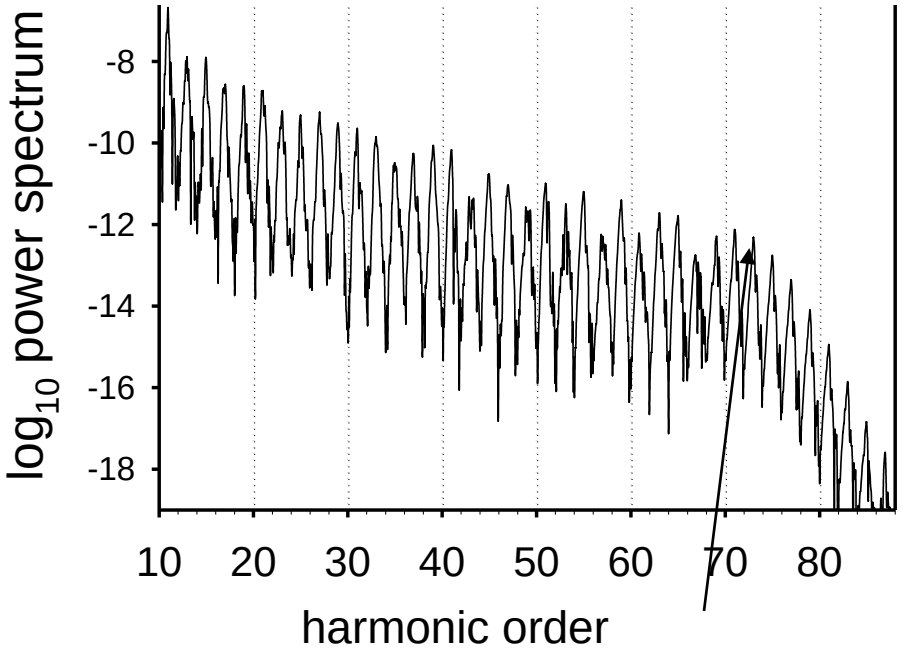

Cuttof at:

$$n_{cut} = [I_p + 3.17\ U_p]/\omega_L\ ,\quad \mathrm{U_p} = \frac{\mathrm{I}/\mathrm{I_{at}}}{4\omega_L^2},$$

$$\mathrm{I_{at}} = 3.51 \times 10^{16}\ \mathrm{W/cm^2}.$$

ADB et al,J Mod Opt 52,411(2005)

(Vo > 0)

Semi-classical model, by P. Corkum (1993).

(Vo =0)

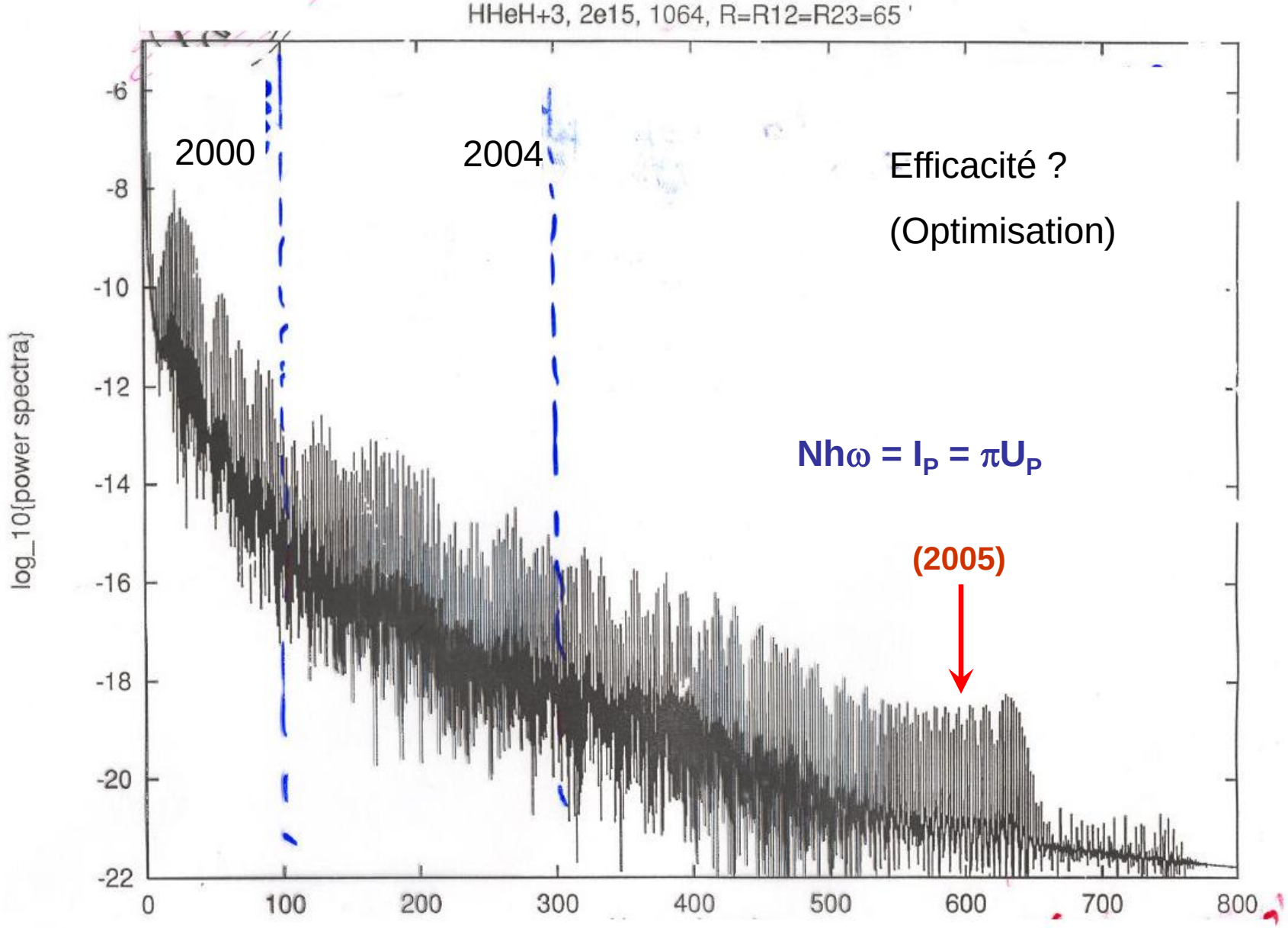

A.D. Bandrauk and H.S. Nguyen, Phys. Rev. A **66**, 031401 (2002)

Step 1: get spectrum

$a(t) = \langle \psi | -\partial V/\partial z \, | \psi \rangle \; -E(t)$

$$a(\omega) = \frac{1}{2\pi} \int_{-\infty}^{+\infty} a(t) e^{-i\omega t} dt$$

Step2: select frequency region between $\omega_1 < \omega < \omega_2$

Step3: come back to time domain

$$\tilde{a}(t) = \int_{\omega_1}^{\omega_2} a(\omega) e^{i\omega t} d\omega$$

$$\Delta\omega = \omega_2 - \omega_1$$

$$\tau \approx \frac{1}{\Delta\omega} \rightarrow \text{attosecond}$$

= 3 Angstroms(10-8cm) / c(3x10**10cm/s-1))**

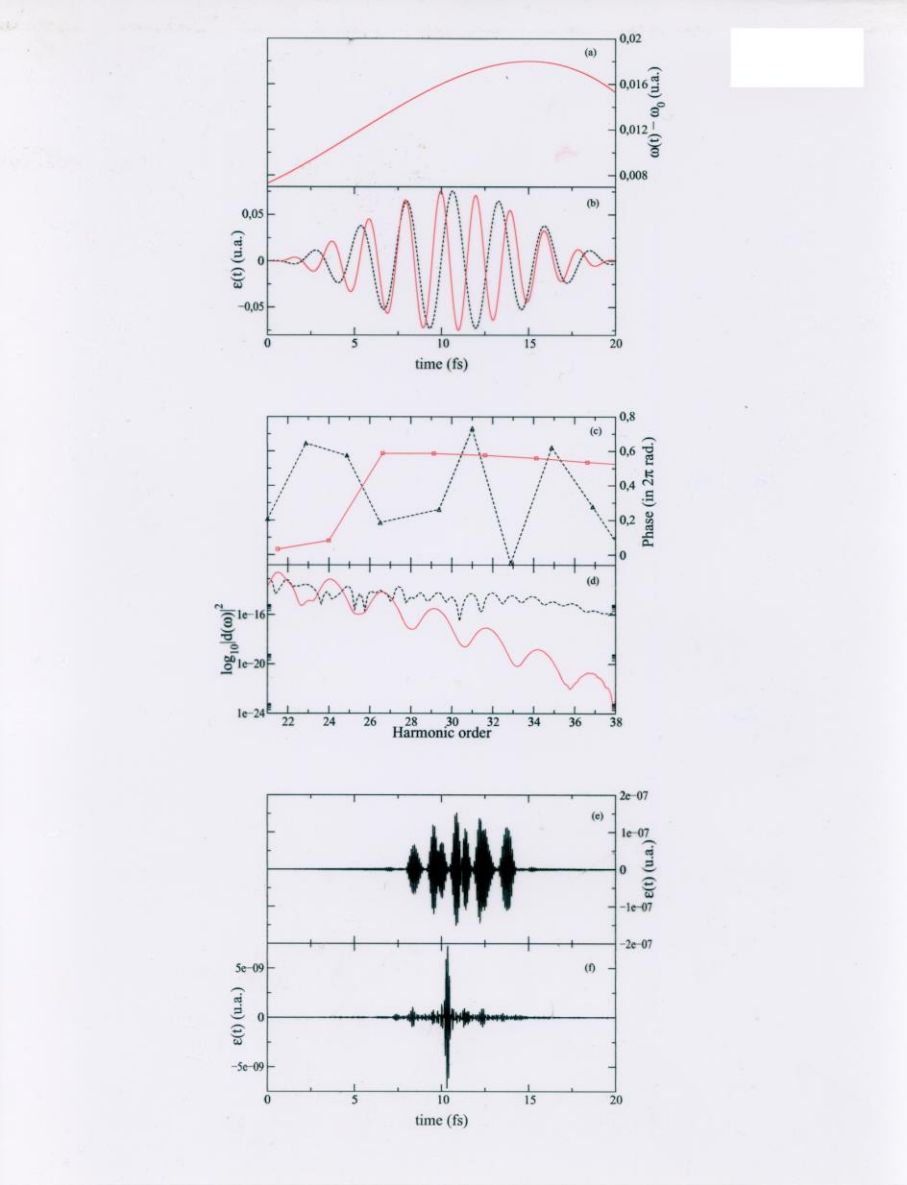

Yedder, LeBris, Chelkowski, Bandrauk, PRA 69, 041802 (2004)

((Bartels.Murrnane.Rabitz.PRA 70.043404(2004))

Frequency-up conversion, 1st -->3rd harmonics

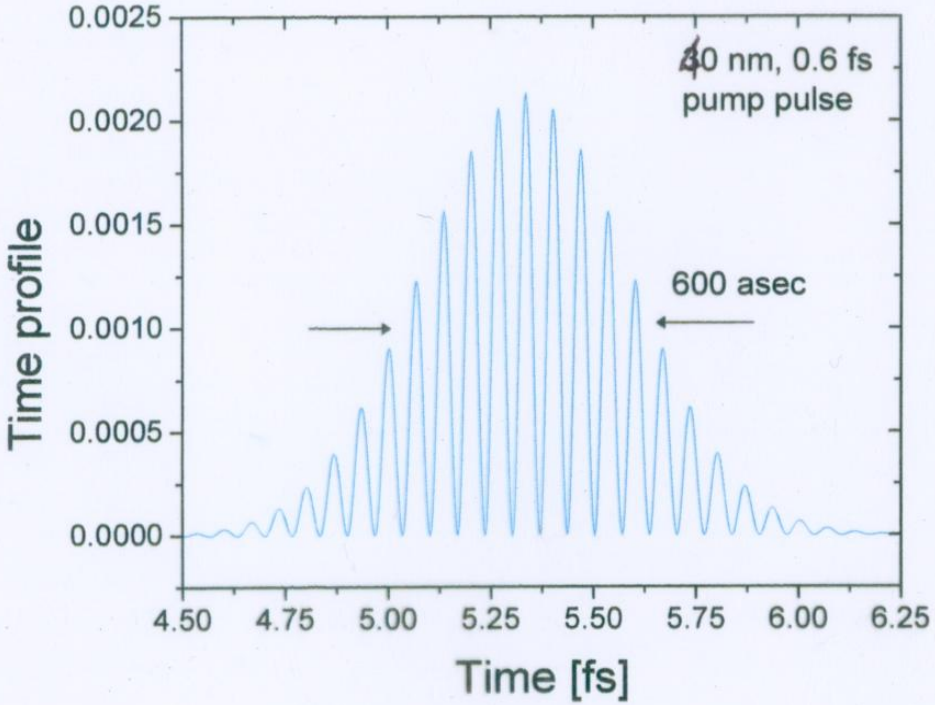

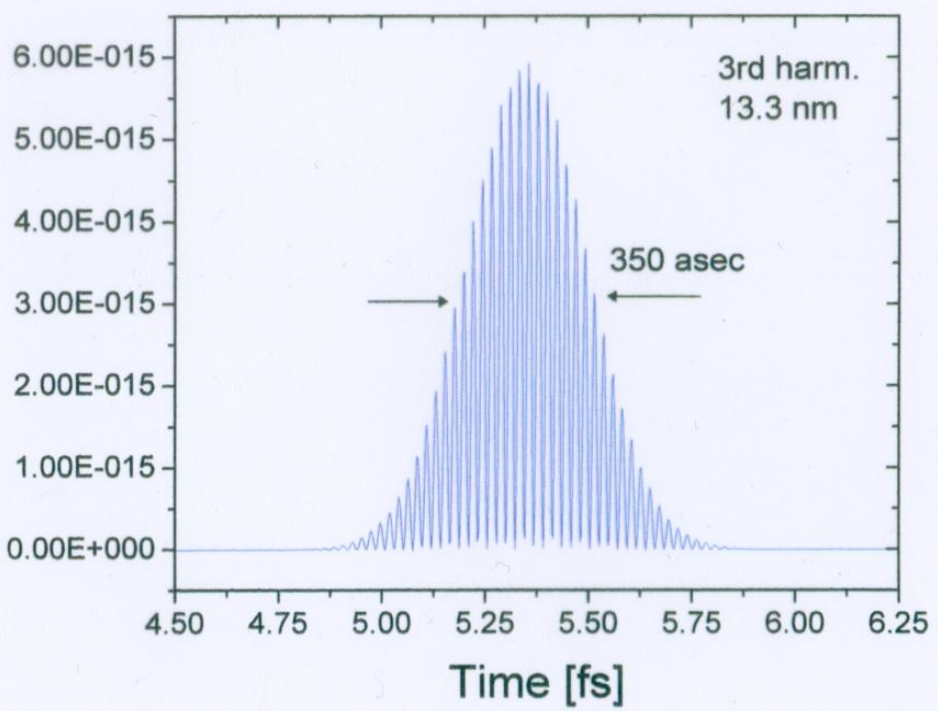

ADB et al,J Molec Str. 735,203(2004)

Goulielmakis,Krausz (2009-2010)

LQ11676

Effect of Nuclear Motion on Molecular High-order Harmonics and on Generation of Attosecond Pulses in Intense Laser Pulses

André D. Bandrauk, Szczepan Chelkowski, Shinnosuke Kawai, and Huizhong Lu

Département de Chimie, Université de Sherbrooke, Sherbrooke, Qc, J1K 2R1 Canada

Abstract

We calculate harmonic spectra and shapes of attosecond pulse trains using numerical solutions of Non-Born Oppenheimer time-dependent Shrödinger equation for 1-D H_2 molecules in an intense laser pulse. A very strong signature of nuclear motion is seen in the time profiles of high order harmonics. In general the nuclear motion shortens the part of the attosecond pulse train originating from the first electron contribution but it may enhance the second electron contribution for longer pulses. The shape of time profiles of harmonics can thus be used for monitoring the nuclear motion.

PACS numbers: 42.65.Ky, 42.65.Re, 42.50.Hz, 32.80.Rm

Phys Rev Lett(2008,)101,153901

J Phys B 42,075602 (2009)

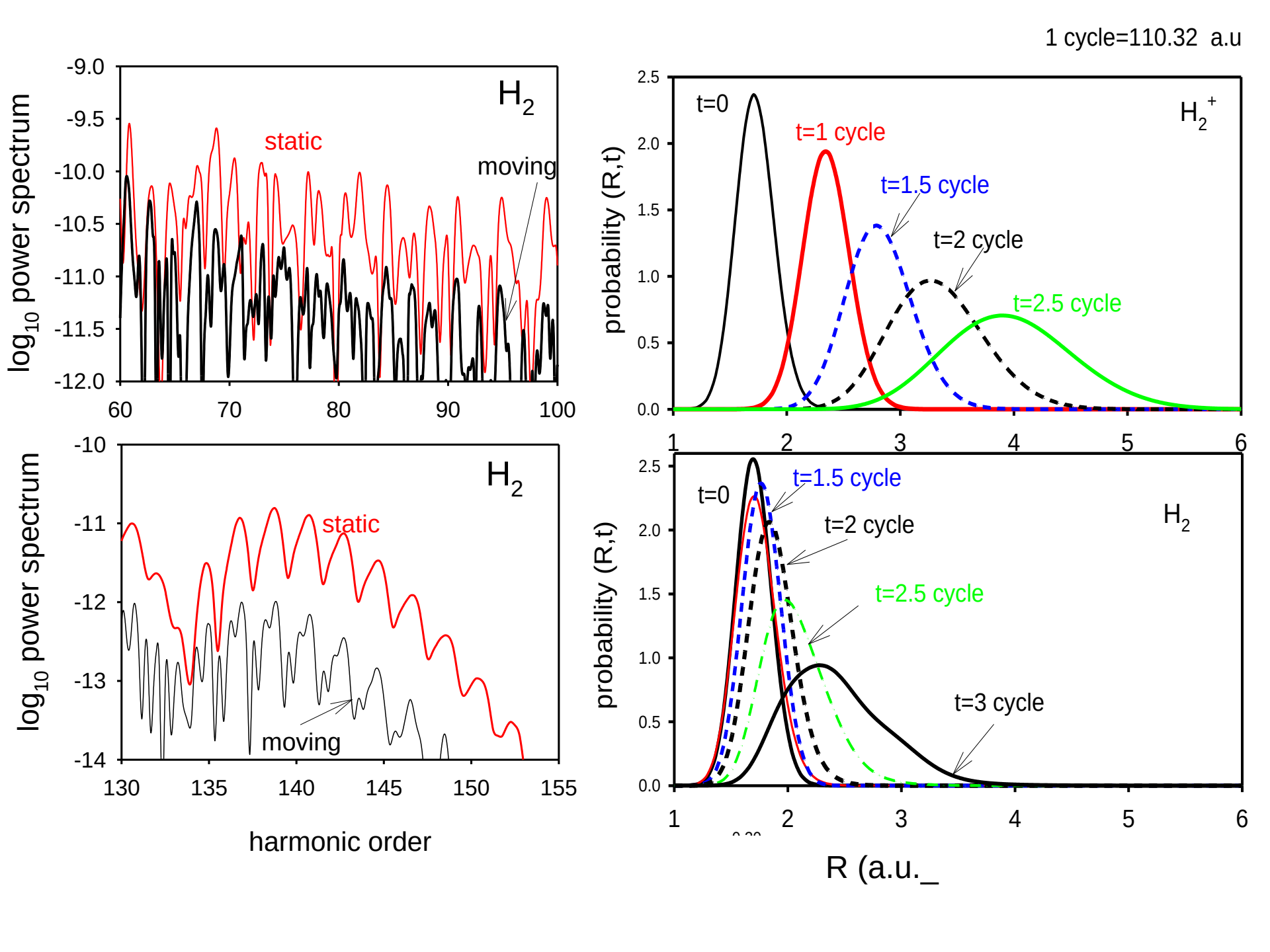
1 cycle=110.32 a.u
H2
static
moving
log10 power spectrum
-9.0
-9.5
-10.0
-10.5
-11.0
-11.5
-12.0
60
70
80
90
100
H2+
t=0
t=1 cycle
t=1.5 cycle
t=2 cycle
t=2.5 cycle
probability (R,t)
2.5
2.0
1.5
1.0
0.5
0.0
1
2
3
4
5
6
H2
static
moving
log10 power spectrum
-10
-11
-12
-13
-14
130
135
140
145
150
155
harmonic order
H2
t=0
t=1.5 cycle
t=2 cycle
t=2.5 cycle
t=3 cycle
probability (R,t)
R (a.u._

Analyse en temps-frequence de Gabor (ondelettes):

$$= d_G(t,\omega) = \int_{-\infty}^{\infty} dt'\, G(t,t')\, \exp(-i\omega t)\, d(t)$$

$$G(t-t') = \exp\left[-\frac{(t-t')^2}{2\sigma_0^2}\right], \quad \sigma_0 = 0.1 \text{ fs}$$

$$d_G(t,\omega) = cte \int_{-\infty}^{\infty} d\omega'\, e^{-b(\omega-\omega')^2}\, e^{i\omega' t}\, d_F(\omega')$$

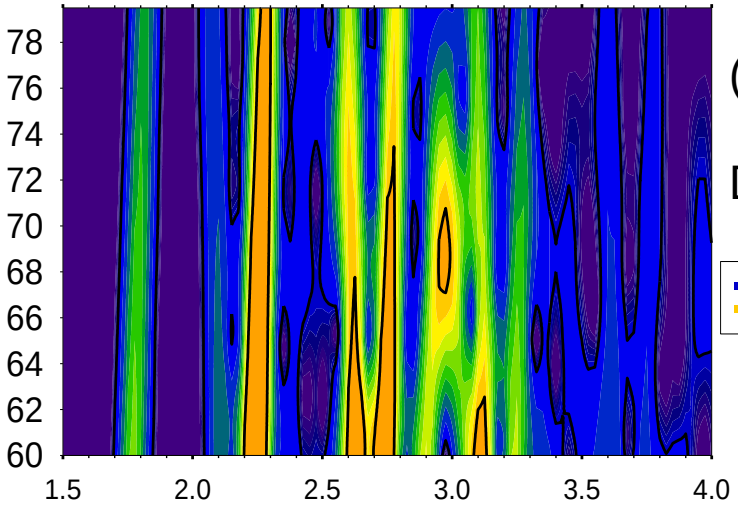

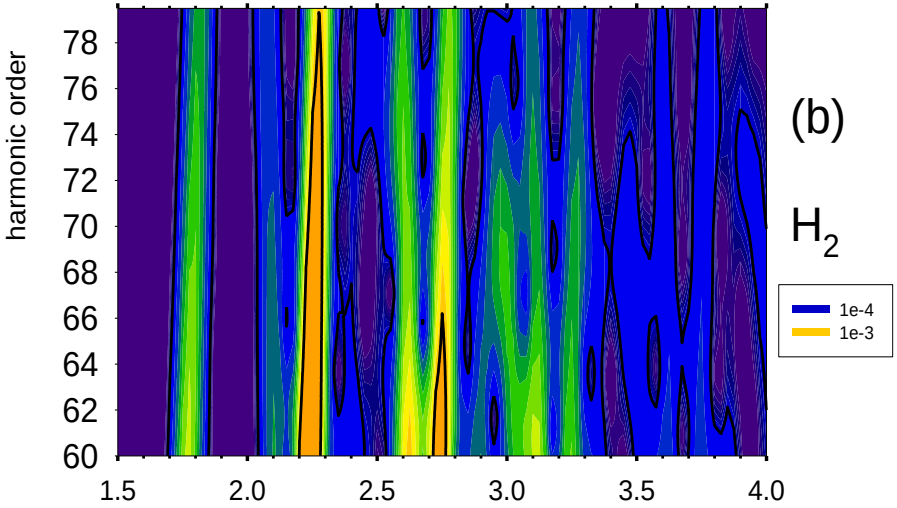

$|d_G(t,\omega)|$ - profile temporaire des impulsions atto dans un train , $\Delta\omega \sim 5\text{-}10\ \omega_L$

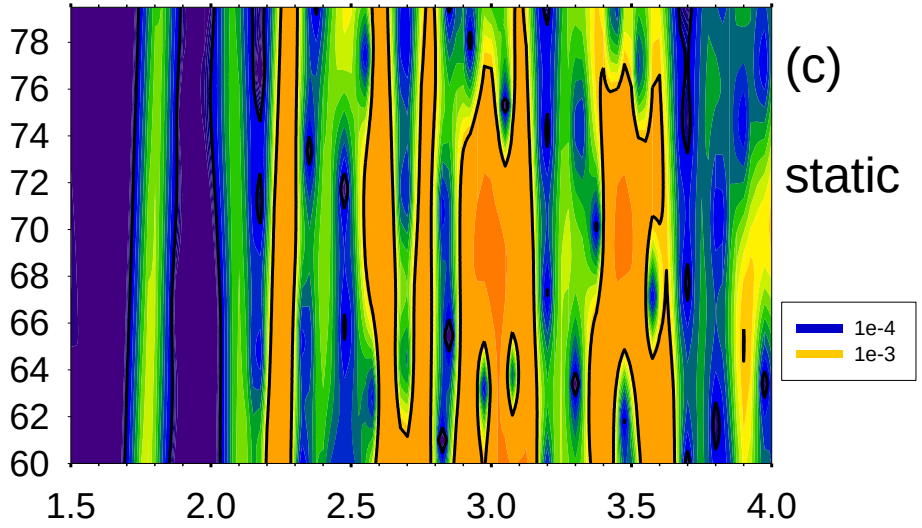

temps (periodes du laser T_{las}) , T_{las}=2.67 fs

Ionized probability density of **HHe^{++}** $2p\sigma\ p_y$

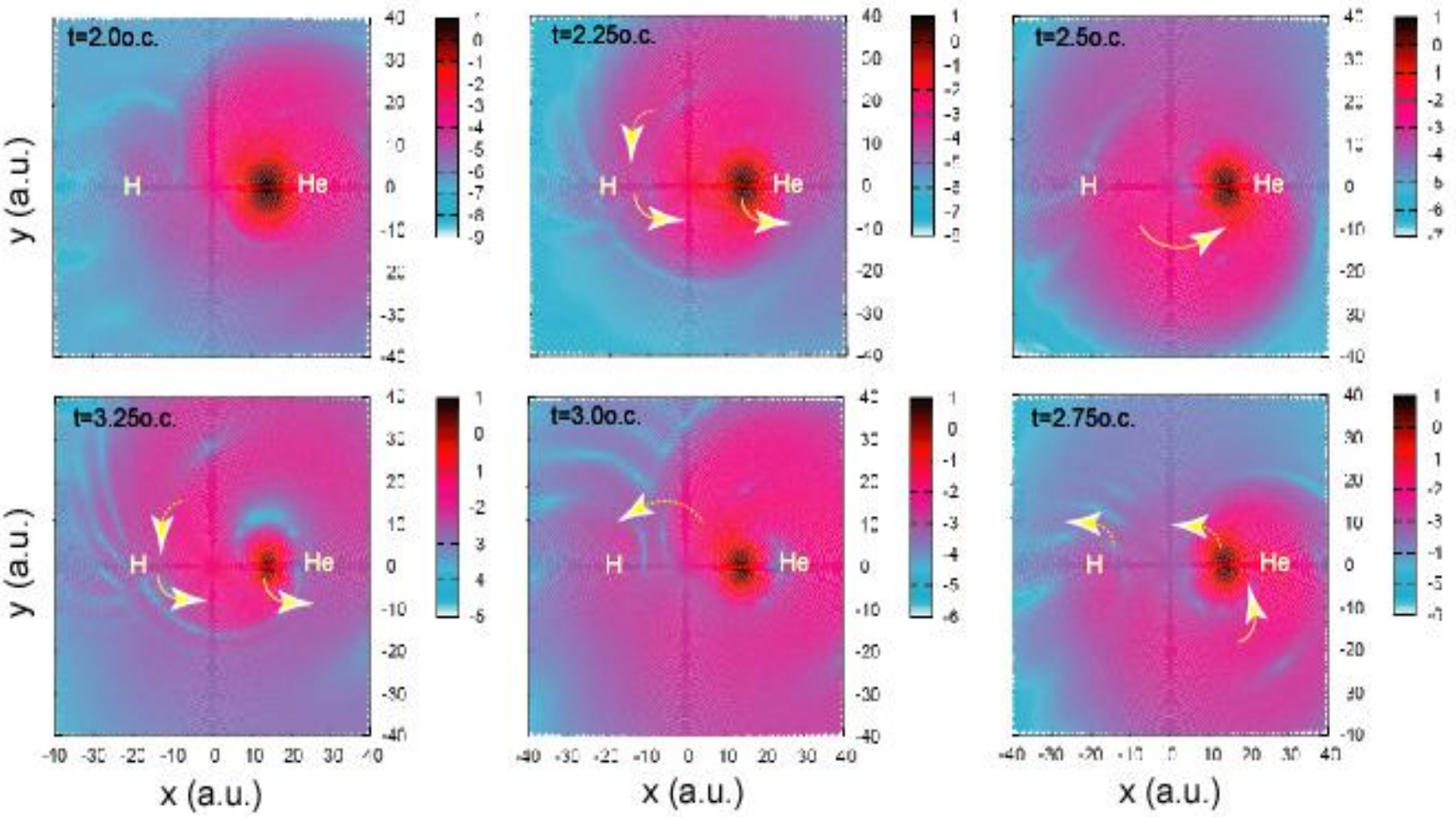

KJ Yuan,ADB,J Phys B –Circular Attosecond Pulses/SPE(2011-1012)

Ellipticity 0.67

HHe^{++} $2p\sigma$ p_y

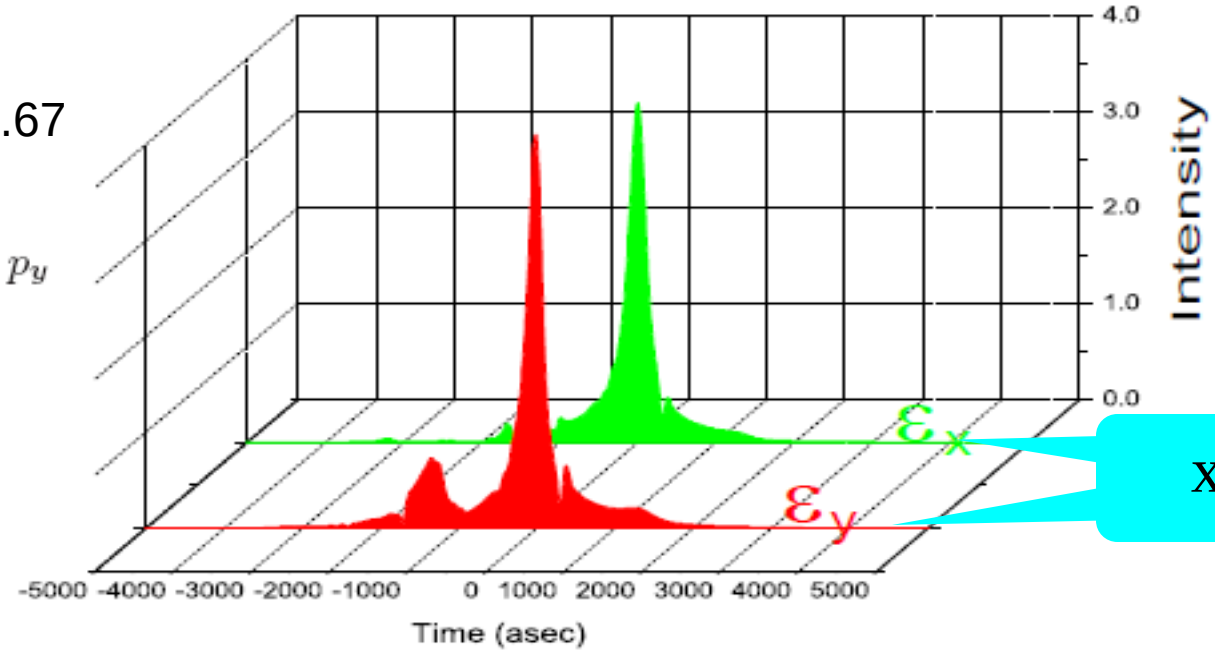

x~y

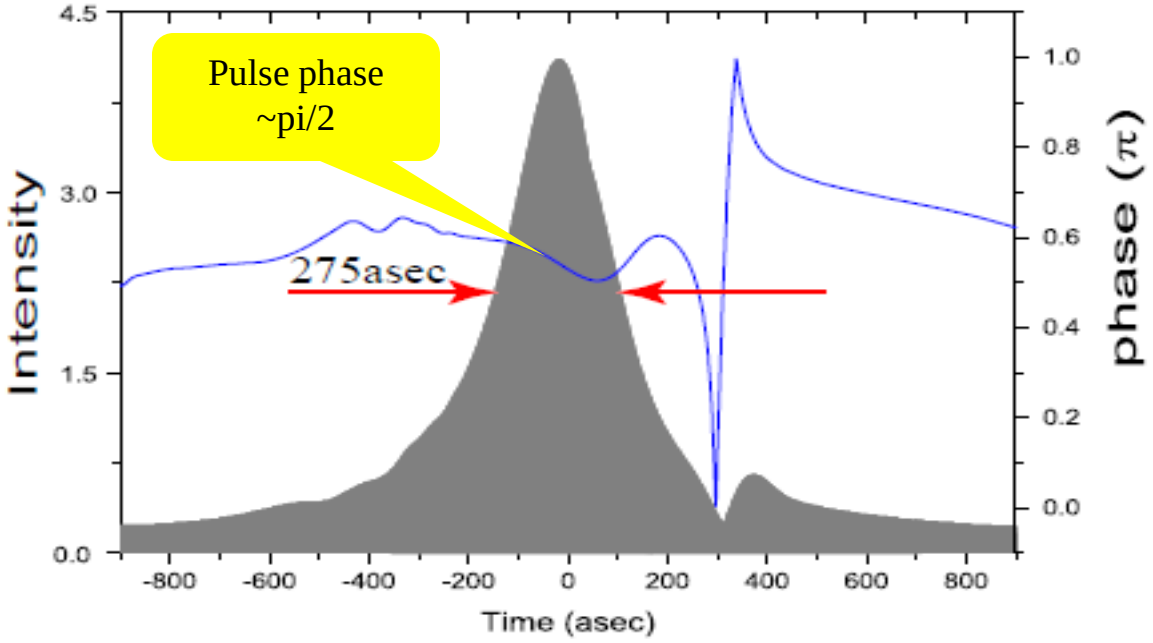

International Journal of Quantum Chemistry

Volume 38 Issue 2, Pages 191 - 208

Published Online: 19 Oct 2004

Article

Theoretical approach to reactions of polyatomic molecules

L. Zülicke, A. Merkel

Akademie der Wissenschaften der DDR, Zentralinstitut für physikalische Chemie, DDR-1199 Berlin, German Democratic Republic

ABSTRACT

A scheme for systematic reduction of the theoretical treatment of elementary reactions involving polyatomic molecules is described; it consists of (1) limitation to the energetically relevant regions of the nuclear configuration space (the reaction path and its near environs) and (2) restriction to the dynamically relevant subspace of the nuclear configuration space (the active modes). Starting from a generalized reaction path Hamiltonian of Nauts and Chapuisat allowing for the use of arbitrary curvilinear coordinates and several large-amplitude modes, the realization of the above-sketched scheme is discussed. A compilation of recent work along these lines, mostly based on the simplified Miller-Handy-Adams reaction path Hamiltonian, is given with particular emphasis on applications of a statistical adiabatic model.

Received: 14 February 1989; Accepted: 4 July 1989

DIGITAL OBJECT IDENTIFIER (DOI)

10.1002/qua.560380214 About DOI

Journal of Physics B: Atomic, Molecular and Optical Physics

Journal of Physics B: Atomic, Molecular and Optical Physics > Volume 39 > Number 13

S Chelkowski *et al* 2006 *J. Phys. B: At. Mol. Opt. Phys.* **39** S409 doi: 10.1088/0953-4075/39/13/S14

Observing electron motion in molecules

S Chelkowski[1], G L Yudin[1,2] and A D Bandrauk[1]

Show affiliations

We study analytically the possibility for monitoring electron motion in a molecule using two ultrashort laser pulses. The first prepares a coherent superposition of two electronic molecular states whereas the second (attosecond pulse) photoionizes the molecule. We show that interesting information about electron dynamics can be obtained from measurement of the photoelectron spectra as a function of the time delay between two pulses. In particular, asymmetries in photoelectron angular distribution provide a simple signature of the electron motion within the initial time-dependent coherently coupled two molecular states. Both asymmetries and electron spectra show very strong two-centre interference patterns. We illustrate these effects using as an example a dissociating hydrogen molecular ion probed by the attosecond pulses.

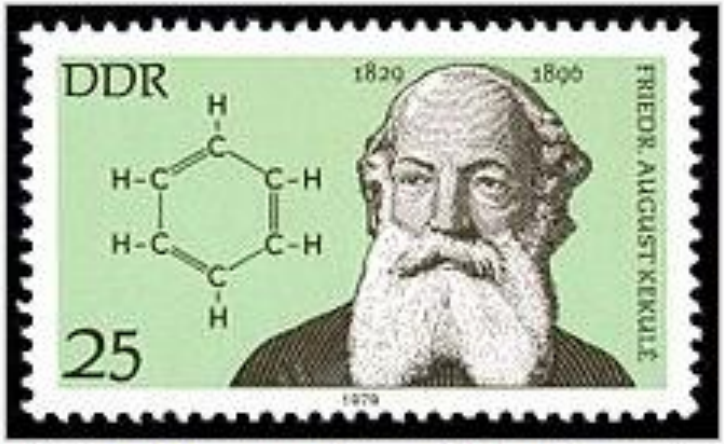

1979 East German stamp of Kekulé, in honour of the sesquicentennial of his birth.

1964 West German centenary stamp for the discovery of the molecular formula of benzene.

Science

Exciting electrons

Chemistry rarely grabs the limelight. But in 2011 it will try to

Nov 22nd 2010 | from PRINT EDITION

One sugar, please

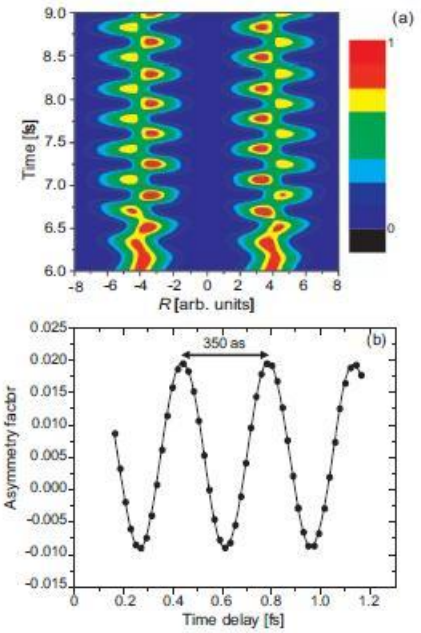

FIG. 53. (Color) Proposal for inducing attosecond electron wave-packet dynamics by a 0.8-fs, 115-nm VUV pump pulse in H_2^+ and probing it with a time-delayed 0.1-fs, 20-nm XUV pulse (Bandrauk *et al.*, 2004). Both pulses are polarized parallel to the molecular axis. (a) Contour plot of the electron probability distribution along the molecular axis for an internuclear distance of eight atomic units vs pump-probe delay. (b) Asymmetry factor $(P_- - P_+)/(P_- + P_+)$ vs delay, where P_+ and P_- represent the probability of observing the electron liberated by the XUV probe in the positive or negative direction (along the molecular axis), respectively. Adapted from Bandrauk *et al.*, 2004.

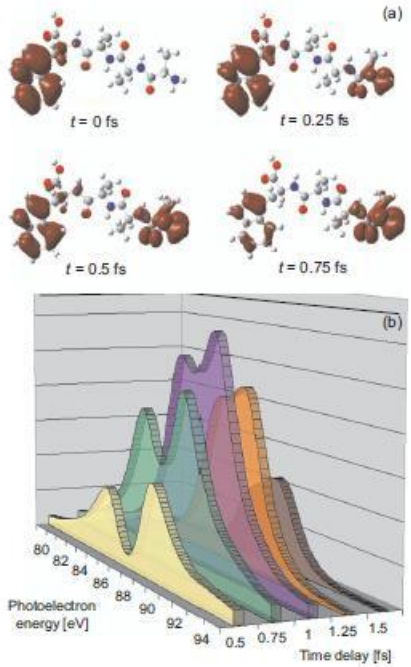

FIG. 54. (Color) Computed ultrafast positive charge (hole) migration in a tryptophane-terminated tetrapeptide (Remacle and Levine, 2006a, 2007). (a) The hole density shown in red indicates that the charge swings across the entire peptide from the aromatic amino acid on the left to the *N* end on the right within less than one femtosecond, following excitation of the electronic wave packet on an attosecond time scale. This hyperfast charge migration is proposed to be probed by measuring the kinetic energy distribution of photoelectrons released by a time-delayed sub-fs XUV pulse. (b) A series of such freeze-frame spectra calculated for a 250-as, 95-eV probe pulse at different pump-probe delays. From Remacle and Levine,

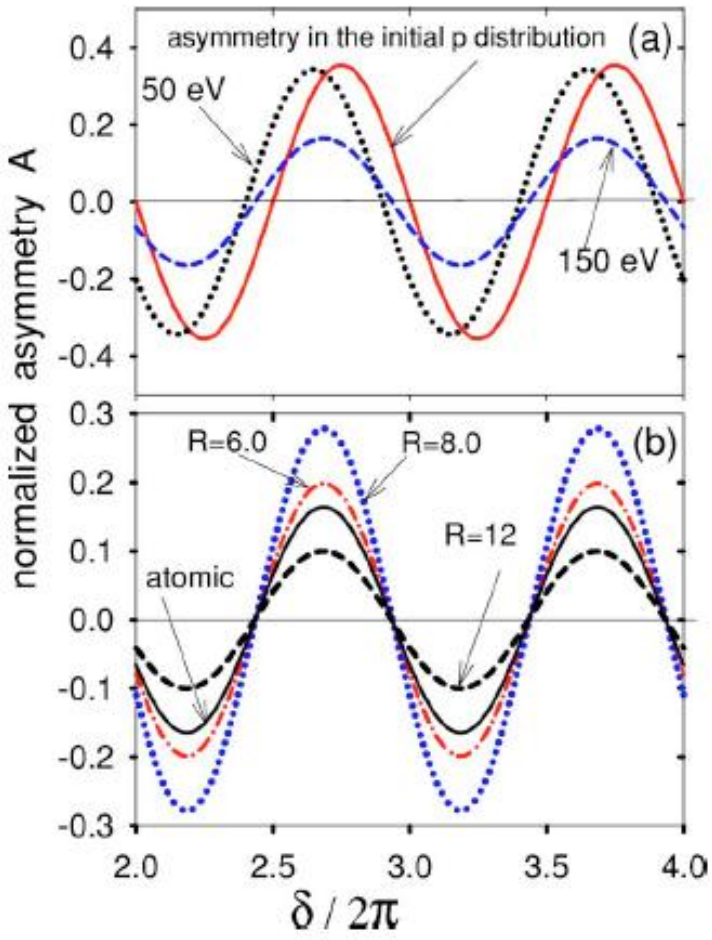

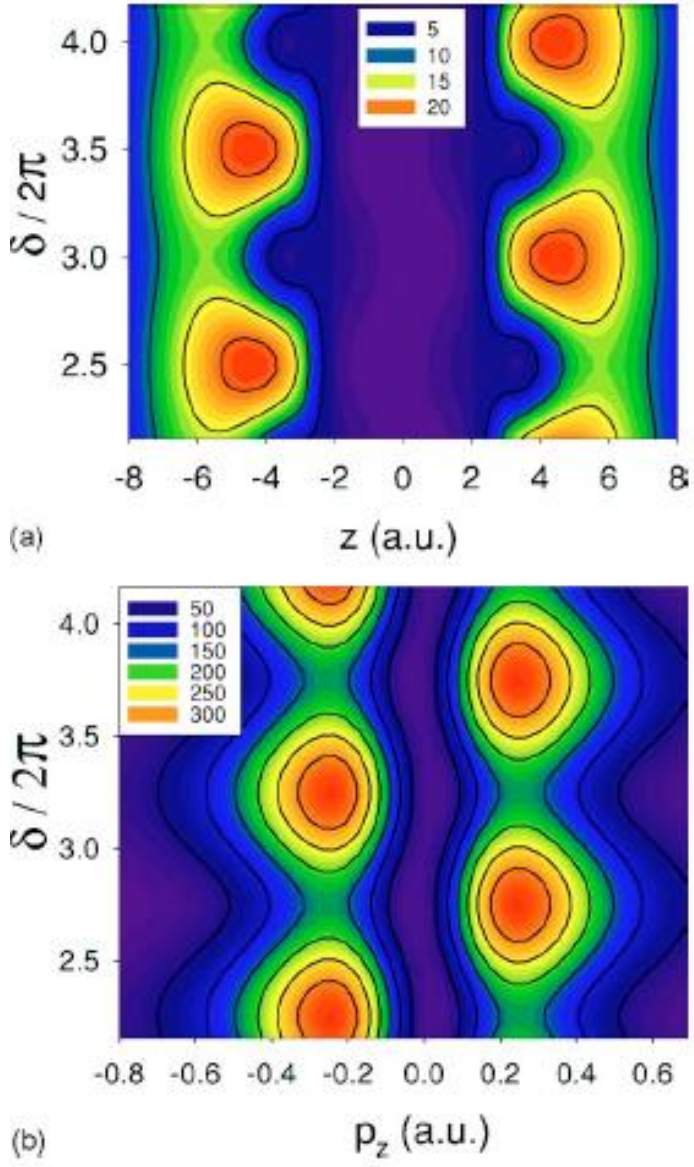

FIG. 2. (Color online) The asymmetries in (a) H atom and (b) H_2^+ molecule (for R=6, 8, and 12 a.u.) as functions of the phase shift δ. The pulse duration is τ_{FWHM}=100 asec. The photon energy and polar angle in Fig. 2(b) are Ω_x=150 eV and θ=30°.

Monitoring Electron Dynamics by (M)HOHG pump probe spectroscopy

T. Bredtmann
Freie Universität Berlin and
Université de Sherbrooke

S. Chelkowski and A. D. Bandrauk
Université de Sherbrooke

(Dated: February 21, 2011)

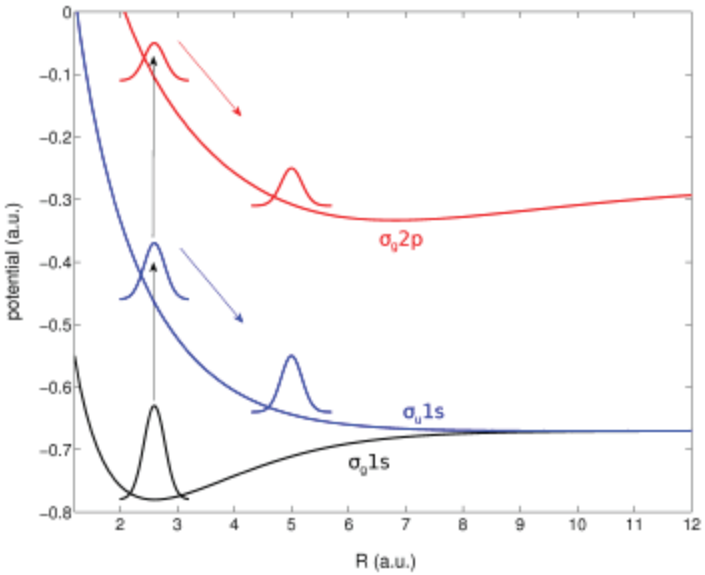

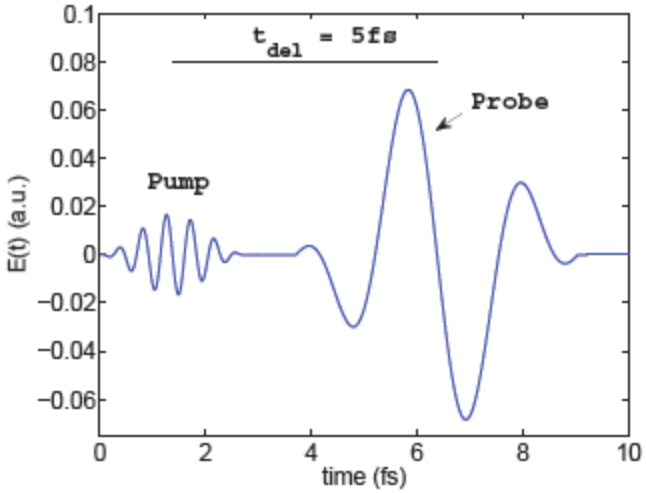

PRA 84,021401(2011)

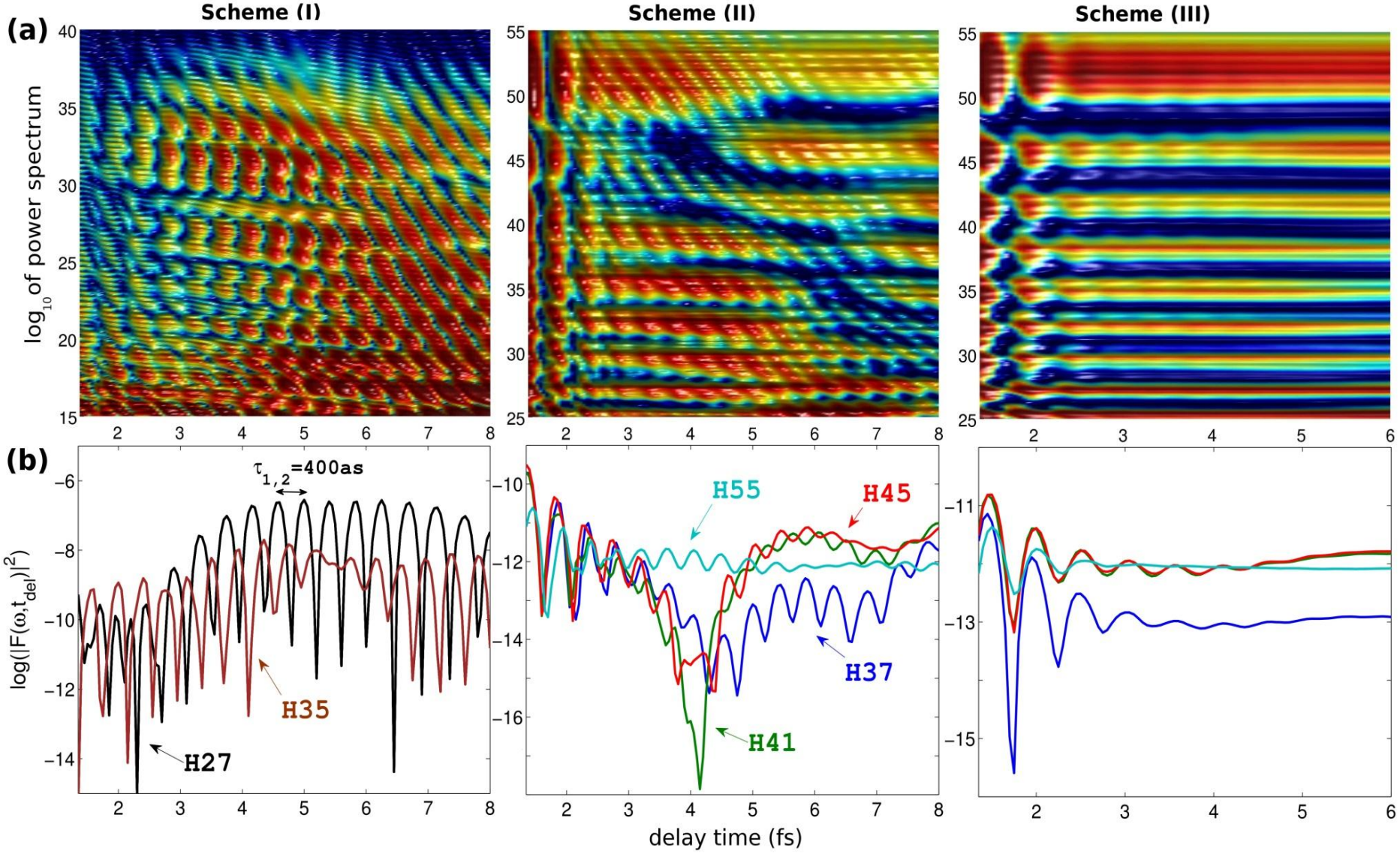
Scheme (I)
Scheme (II)
Scheme (III)
(a)
log10 of power spectrum
(b)
log(|F(ω,tdel)|2)
τ1,2=400as
H27
H35
H55
H45
H37
H41
delay time (fs)

$I_{pump}=10^{13}$ W/cm^2 + $I_{probe}=2\times10^{14}$ W/cm^2 , $\omega_{pump}=0.28$ a.u

very strong two-photon resonance from σ_u1s to σ_g2p

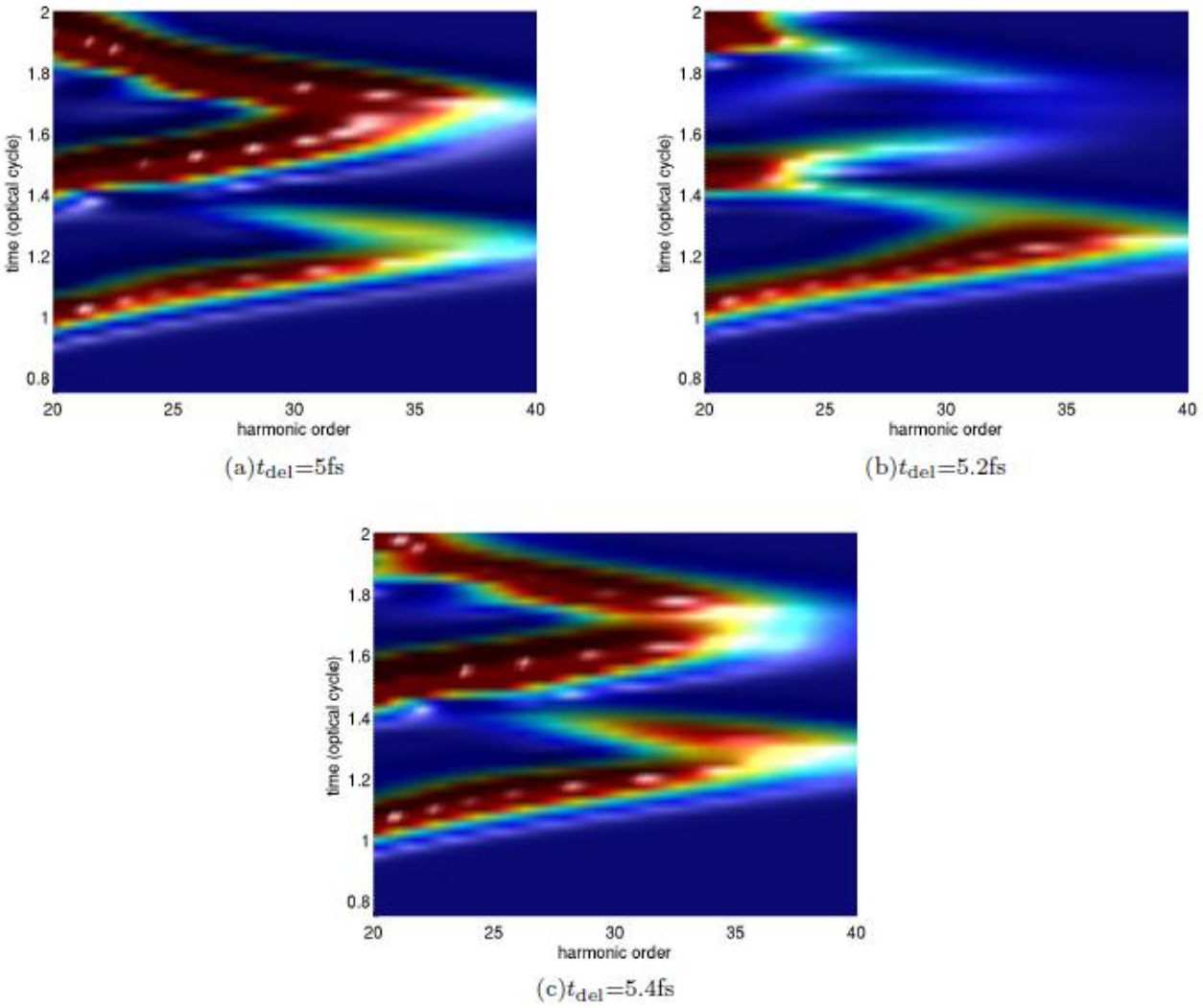

(a)t_{del}=5fs (b)t_{del}=5.2fs

(c)t_{del}=5.4fs

FIG. 7. Wavelet time-frequency spectrum for different delay times: t_{del}=5fs (a), t_{del}=5.2fs (b), t_{del}=5.4fs (c).

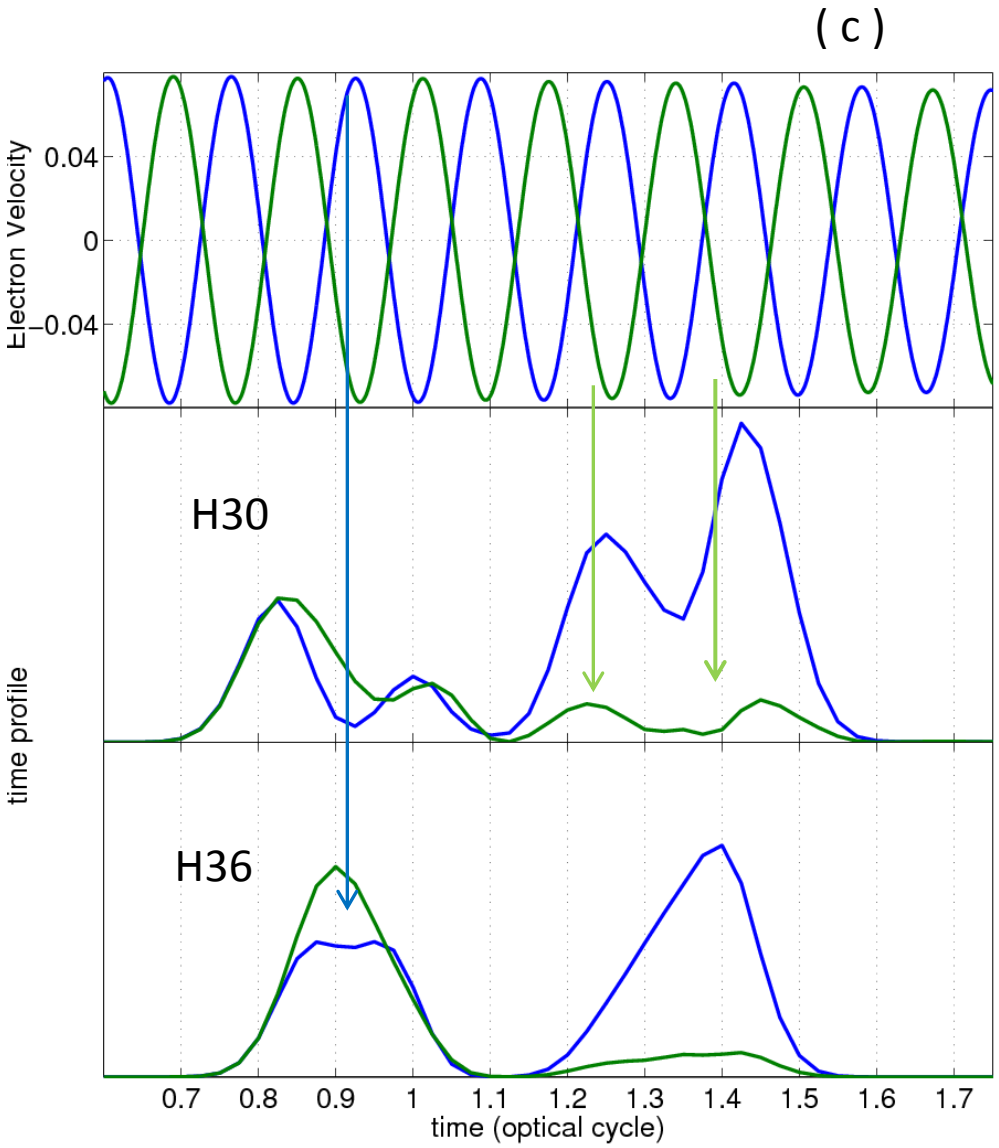

Fig.4 Time-profiles for the scheme (I) , blue - t_{del}=5.0, green- t_{del}=5.2fs

HeH++

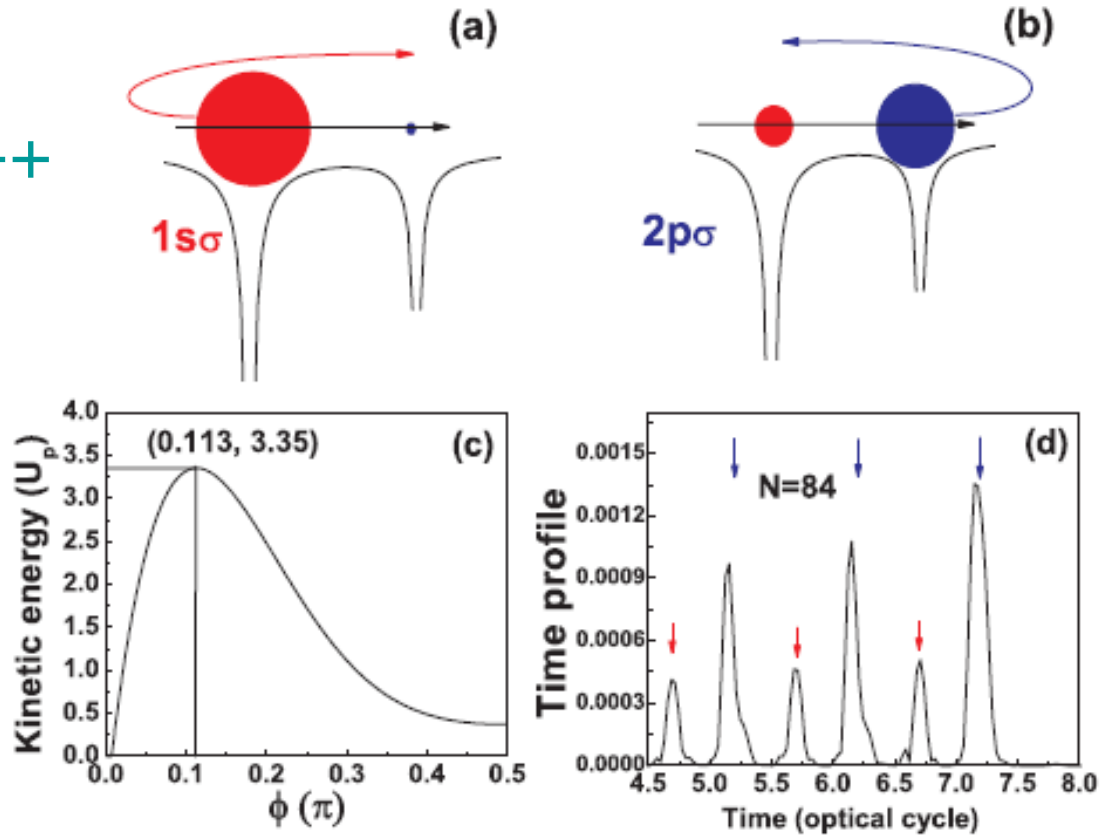

FIG. 3 (color online). (a) and (b) is schematic illustration of collision processes of $1s\sigma$ and $2p\sigma$ states from one well to the other well. (c) is the collision kinetic energy of electron obtained from the laser field as a function of the phase when it is ionized. (d) is the time profile of harmonics order 84 of Fig. 1(a). The arrows correspond to the collision time from 1D classical model.

X.B. Bian and A.D. Bandrauk Phys. Rev. Lett. **105**, 093903 (2010)

Springer
The language of science

springer.com

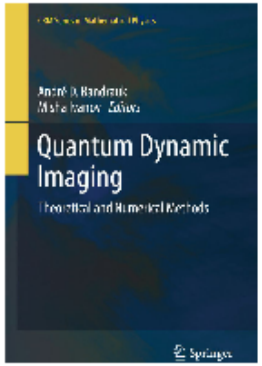

233 pages
79 illus., 76 in color
Hardcover
ISBN 978-1-4419-9490-5
$129.00

Forthcoming
May 2011

CRM Series in
Mathematical Physics

CENTRE
DE RECHERCHES
MATHÉMATIQUES

Quantum Dynamic Imaging

Theoretical and Numerical Methods

Editors:
André D. Bandrauk, Université de Sherbrooke, QC, Canada
Misha Ivanov, Imperial College London, UK

Studying and using light or "photons" to image and then to control and transmit molecular information is among the most challenging and significant research fields to emerge in recent years. One of the fastest growing areas involves research in the temporal imaging of quantum phenomena, ranging from molecular dynamics in the femto (10^{-15}s) time regime for atomic motion to the atto (10^{-18}s) time scale of electron motion. In fact, the attosecond "revolution" is now recognized as one of the most important recent breakthroughs and innovations in the science of the 21st century. A major participant in the development of ultrafast femto and attosecond temporal imaging of molecular quantum phenomena has been theory and numerical simulation of the nonlinear, non-perturbative response of atoms and molecules to ultrashort laser pulses. Therefore, imaging quantum dynamics is a new frontier of science requiring advanced mathematical approaches for analyzing and solving spatial and temporal multidimensional partial differential equations such as Time-Dependent Schroedinger Equations (TDSE) and Time-Dependent Dirac equations (TDDEs for relativistic phenomena). These equations are also coupled to the photons in Maxwell's equations for collective propagation effects. Inversion of the experimental imaging data of quantum dynamics presents new mathematical challenges in the imaging of quantum wave coherences on subatomic (subnanometer) spatial dimensions and multiple timescales from atto to femto and even nanoseconds.

In ***Quantum Dynamic Imaging: Theoretical and Numerical Methods***, leading researchers discuss these exciting state-of-the-art developments and their implications for R&D in view of the promise of quantum dynamic imaging science as the essential tool for controlling matter at the molecular level.

Key Features:

- Presents the latest research results in ultrafast imaging of quantum phenomena
- Demonstrates the wide-ranging potential of quantum dynamic imaging for R&D in areas as diverse as optoelectronics, materials science, and quantum information
- Edited and written by international leaders in the field

➢ **Table of Contents and Order Form on Reverse**

Imaging and Controlling Molecular Dynamics with Ultrashort Laser Pulses

Friday, February 17, 2012: 8:00 AM-9:30 AM
Room 208-209 (VCC West Building)

Ten years ago, A.H. Zewail was awarded the Nobel prize for "femtosecond" chemistry, monitoring atomic motion in chemical reactions with femtosecond(fs) pulses. Modern laser technology generates attosecond (asec) pulses for studying electron motion on its own time-scale. Attosecond science is now considered a major breakthrough in the science of the 21st century. Free electron lasers (FELs) are adding more tools for the study of ultra-fast quantum dynamics in matter with coherent light sources from the near infrared to ultra-short X-ray wavelengths. Chemical, biological, and material sciences have spent over a century on elucidating and relating molecular structures to molecular function. New ultra-short laser pulses are now becoming the essential tools for imaging, visualizing, and controlling ultra-fast asec electron dynamics coupled to fs nuclear dynamics in molecules in such processes as vision, photosynthesis, electron transfer, and so on. The symposium will begin with a review of the issues in measuring coherent electron motion and transfer in photexcitations of complex molecules. Other presentations will deal with new developments and applications of ultra-short laser pulses and coherent FEL sources to measuring, imaging, and controlling ultra-fast quantum dynamics in matter, thus heralding the emergence of a new science: Femto-Attosecond Science.

Organizer: *Andre D. Bandrauk, Universite de Sherbrooke*
Co-Organizer: *Paul B. Corkum, University of Ottawa*
Moderator: *Andre D. Bandrauk, Universite de Sherbrooke*
Discussants: *Andre D. Bandrauk, Universite de Sherbrooke and Paul B. Corkum, University of Ottawa*
Speakers:

***Margaret Murnane**, University of Colorado*
Advances in Ultrafast Laser Technology: Femto to Attosecond Science

***Graham R. Fleming**, University of California*
Ultrafast Laser Measurements of Coherences and Entanglement in Light-Harvesting Systems

***John C.H. Spence**, Arizona State University*
X-Ray and FELUltrafast Sources in Protein and Virus Imaging from Structure to Function

AAAS ADVANCING SCIENCE, SERVING SOCIETY
Annual Meeting
16-20 February 2012 • Vancouver, Canada
Start | Speaker Index

Understanding Cellular Machinery Through X-Ray Imaging

Friday, February 17, 2012: 10:00 AM-11:30 AM
Room 208-209 (VCC West Building)

What does the world of viruses, bacteria, and cells look like? For years, our understanding of the structure and function of these biological systems has been transformed by a single technology: protein crystallography. In this technique, proteins are removed from their environment, crystallized, and interrogated by X-rays to obtain their static structure. With new imaging technologies, scientists can obtain sharp, clear images of living, dynamic structures in their native environments. X-ray tools are opening frontiers in understanding the reactions happening inside cells by understanding cellular life. This symposium will explore three tools that open vistas, allowing direct visualization and quantitative analysis of the cellular machinery. These technologies bring, tantalizingly close, the possibilities of imaging individual biological molecules that are too small to study, even with the most powerful microscopes.

Organizer: *Louis J. Terminello, Pacific Northwest National Laboratory*
Speakers:

***Henry N. Chapman**, Center for Free-Electron Laser Science*
Imaging and Nanocrystallography of Biological Objects with X-Ray Free-Electron Lasers

***Carolyn Larabell**, Lawrence Berkeley National Laboratory*
X-Ray Microscopy and the View Inside Living Cells

***Chris Jacobsen**, Advanced Photon Source*
X-Ray Microscopy in Color: 3D Views of Cellular Chemistry

Phys. Rev. Lett. 106, 018301 (2011) [4 pages]

Relativity and the Lead-Acid Battery

Abstract | References | Citing Articles (7) | Supplemental Material

Download: PDF (407 kB) Export: BibTeX or EndNote (RIS)

Rajeev Ahuja[1,*], Andreas Blomqvist[1], Peter Larsson[1], Pekka Pyykkö[2,†], and Patryk Zaleski-Ejgierd[2,‡]

[1]*Division of Materials Theory, Department of Physics and Astronomy, Uppsala University, Box 516, SE-751 20, Uppsala, Sweden*

[2]*Department of Chemistry, University of Helsinki, Box 55 (A. I. Virtasen aukio 1), FI-00014 Helsinki, Finland*

Received 30 August 2010; published 5 January 2011

See accompanying *Physics* Focus

The energies of the solid reactants in the lead-acid battery are calculated *ab initio* using two different basis sets at nonrelativistic, scalar-relativistic, and fully relativistic levels, and using several exchange-correlation potentials. The average calculated standard voltage is 2.13 V, compared with the experimental value of 2.11 V. All calculations agree in that 1.7–1.8 V of this standard voltage arise from relativistic effects, mainly from PbO_2 but also from $PbSO_4$.

High-Energy QED: Real and Virtual Pairs

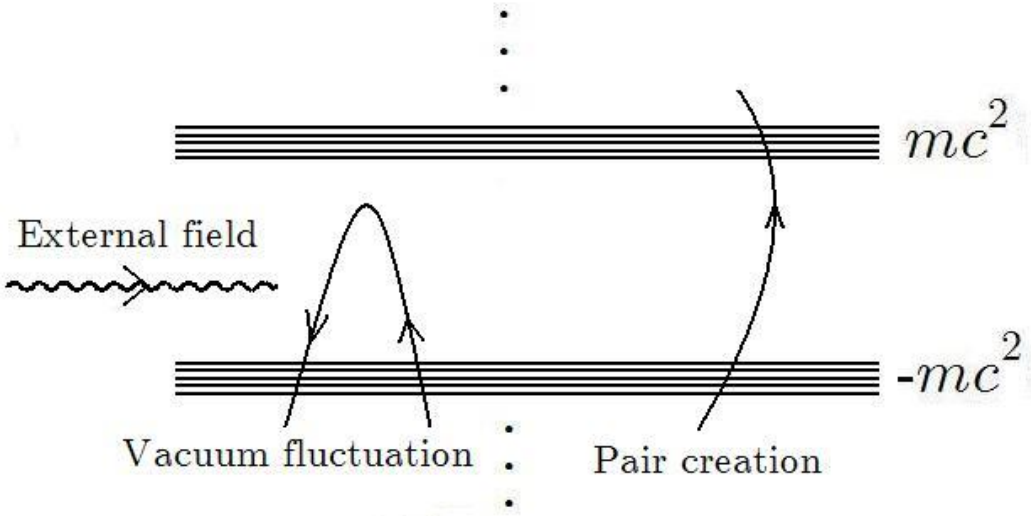

Courtesy of

CH Keitel(MPI,hdb)

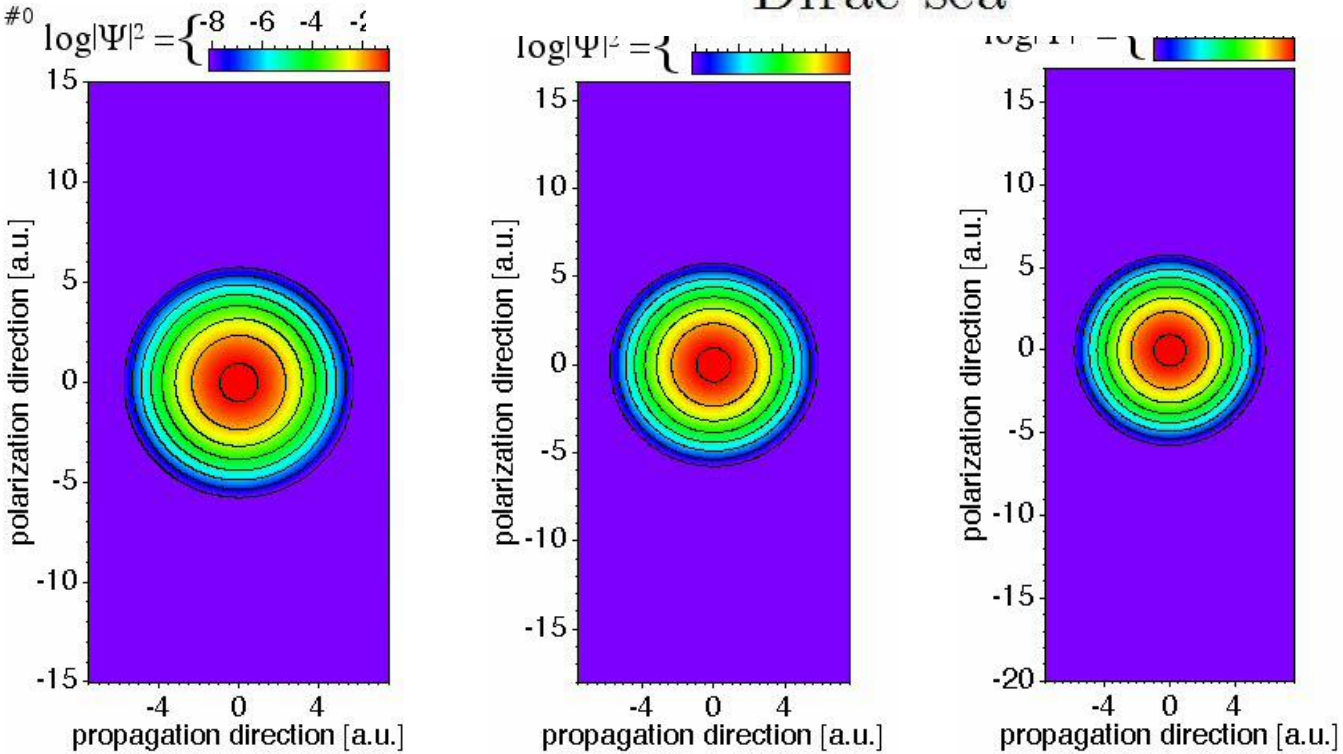

Dirac dynamics of an electron with negative energy in crossed laser beams: pairs from 10^{26} W/cm²

Nonlinear Analysis: Real World Applications 12 (2011) 190–202

Contents lists available at ScienceDirect

Nonlinear Analysis: Real World Applications

journal homepage: www.elsevier.com/locate/nonrwa

A simple and accurate mixed P^0–Q^1 solver for the Maxwell–Dirac equations

E. Lorin [a,*], A. Bandrauk [b]

[a] School of Mathematics and Statistics, Carleton University, Ottawa, K1S 5B6, Canada

[b] Laboratoire de chimie théorique, Faculté des Sciences, Université de Sherbrooke, Sherbrooke, J1K 2R1, Canada

ARTICLE INFO

Article history:
Received 12 May 2010
Accepted 3 June 2010

Keywords:
Maxwell equations
Dirac equation
Laser–gas interaction
Finite element method
Hyperbolic systems

ABSTRACT

In this paper we propose and analyze a simple but accurate numerical method for solving the Maxwell–Dirac system for relativistic particles submitted to an external ultrashort intense pulse. Maxwell's equations are solved using a second order finite element method in space and time. The Dirac equation solver is based on a method of characteristics with a P^0 formulation of the Dirac spinor field. Numerical simulations are provided to show the efficiency of the method.

Mathematical Problems

1. High order SOM
2. Multiscale time frequency analysis
3. Infinite D Optimal Control theory
   (Bartels,Murnane,Rabitz,PRA 70,043404(2004) ;ADB et al,PRA 69,041802(2004))
4. High order NLSE
5. Relativistic QM
6. Molecular movies
   (Dynamic Imaging of Electrons-Nuclei)

SCIENCE / TECHNOLOGY

APRIL 13, 2009 | VOLUME 87, NUMBER 15 | PP. 50-51
ACS MEETING NEWS

Tracking Electrons

Attosecond science opens the door to real-time observation and control of electron dynamics

Jyllian Kemsley

TEN YEARS AGO, Ahmed H. Zewail won the Nobel Prize for using femtosecond spectroscopy to study atomic motions during chemical reactions. Emerging now from Zewail's pioneering work is the ability to use femtosecond laser pulses to monitor attosecond-scale electron dynamics, which was the focus of a Divison of Physical Chemistry symposium on attosecond science at the American Chemical Society national meeting in Salt Lake City last month.

"There's a whole class of processes associated with electron dynamics that occur at a femtosecond timescale or less," Daniel M. Neumark, a chemistry professor at the University of California, Berkeley, said at the meeting. "These are electron dynamics processes that don't require nuclear motion. To probe them you need attosecond-scale pulses."

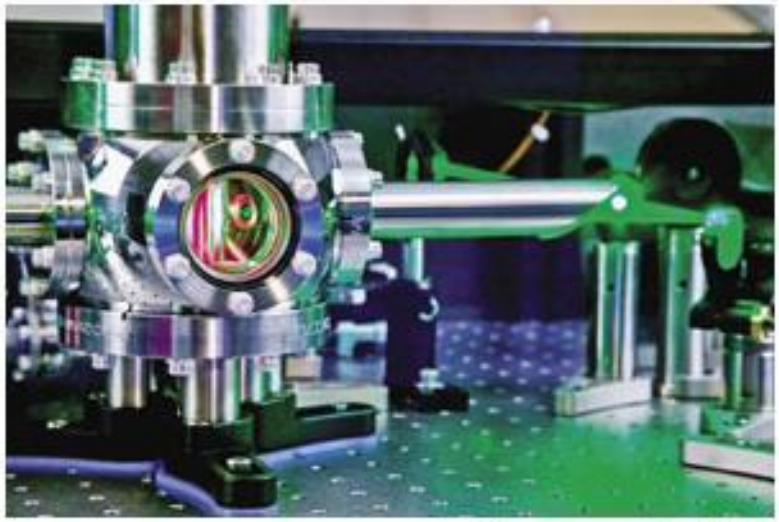

Gary Larson © 2004

ULTRAFAST A cryostat contains a cooled Ti:sapphire laser amplifier crystal that is used to generate high-power femtosecond pulses for attosecond experiments.

Dimérisation de la thymine dans l'ADN par la lumière

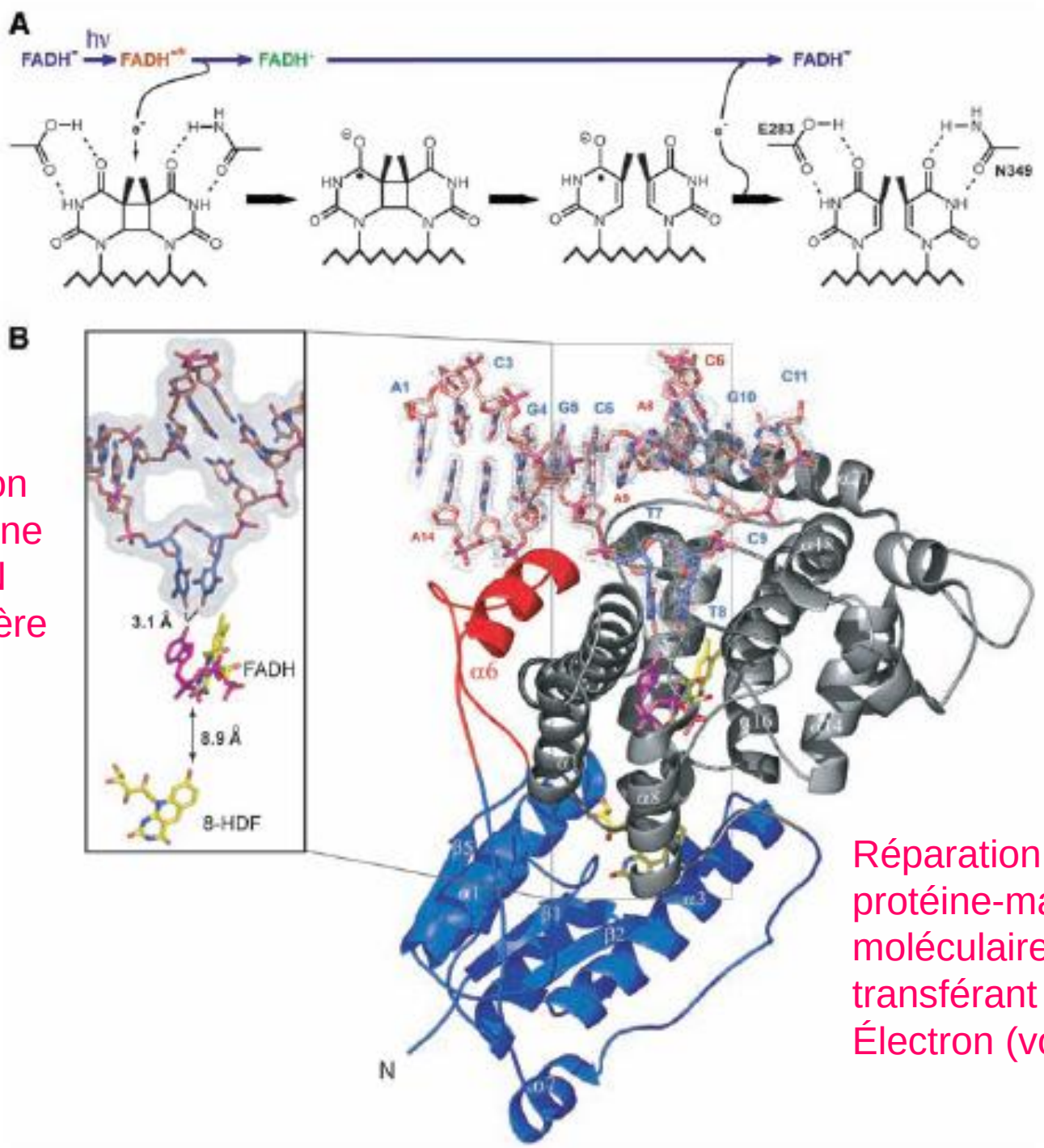

Réparation par une protéine-machine moléculaire en transférant un Électron (voir en haut)

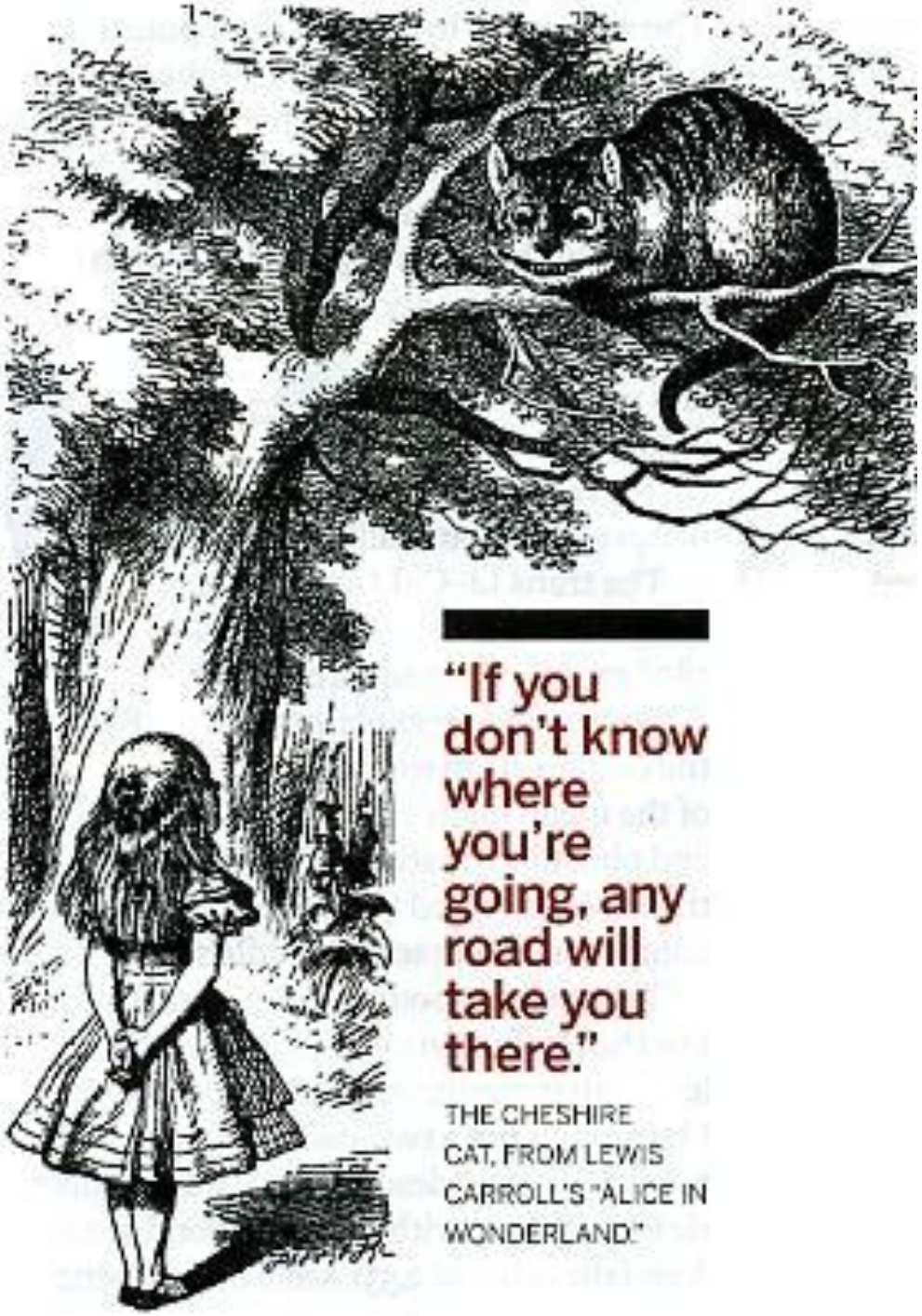

"If you don't know where you're going, any road will take you there."

THE CHESHIRE CAT, FROM LEWIS CARROLL'S "ALICE IN WONDERLAND."

RECOLLISION OF d^+ WITH A μd ATOM INITIATED BY A SUPER-INTENSE LASER

3 U_P **Recollision energy=** 1.40 MeV

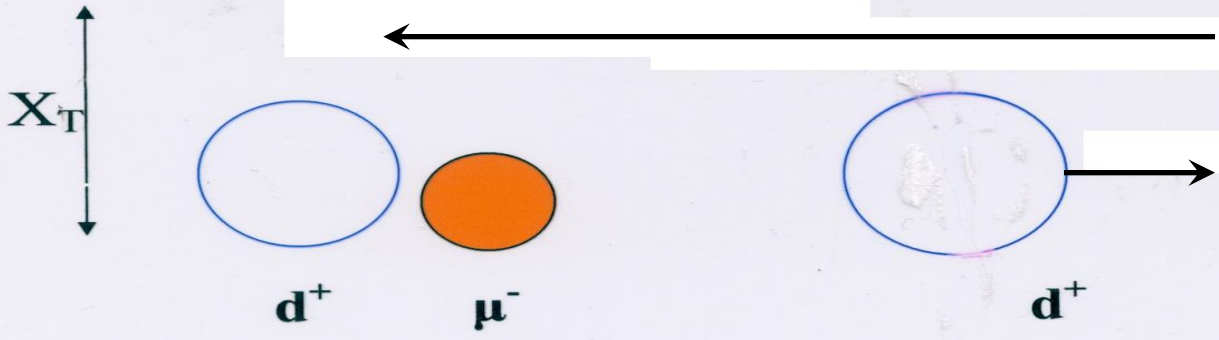

$X_T = 0.9$ Å

ELECTRIC FIELD E(t) OF THE LASER

λ = 800 nm

THUS THE LASER CAN INITIATE

A NUCLEAR REACTION ,e.g: I – 3 x 10^{22} W/cm^2

d +d → n (2.45 MeV)+^{3}He (0.82 Mev)

or

d +t → n (14.1 MeV)+^{4}He (3.5 MeV)

d-μ-d molecule dissociating in
200 nm, I=10^{22} W/cm^2 laser field

deuterium returns back !

E~1/2 MeV

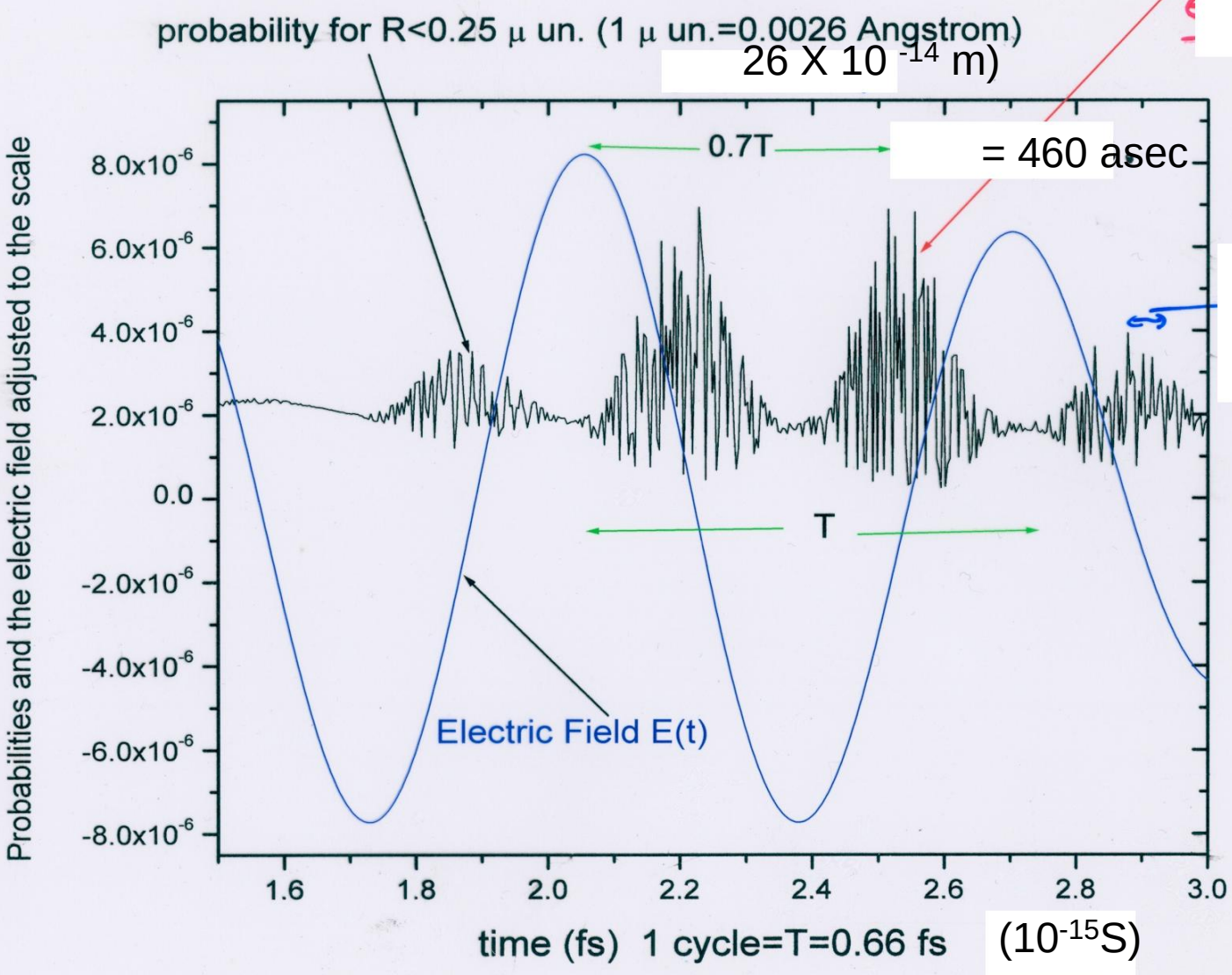

Δt~10^{-18}S

=attosecond

(10^{-15}S)

PRL 93,083602(2004)

Where the "Laser" has never been (2009)

Gérard Mourou

École polytechnique (Fr)

λ= 800 nm

I=3,5 x 10^{26} W/cm^2

$$U_p(e^-) = \frac{I}{4m_e\omega^2} = 20\ TeV$$

$$U_p(\mu^\pm) = 100\ GeV = 0{,}1\ TeV$$

$$U_p(p^\pm) = 10\ GeV$$

$\frac{mc^2}{}$

0,5 MeV

0,1 GeV

1 GeV

Nuclear fusion from explosions of femtosecond laser-heated deuterium clusters

T. Ditmire, J. Zweiback, V. P. Yanovsky, T. E. Cowan, G. Hays & K. B. Wharton

Laser Program, L-477, Lawrence Livermore National Laboratory, Livermore, California 94550, USA

As a form of matter intermediate between molecules and bulk solids, atomic clusters have been much studied[1]. Light-induced processes in clusters can lead to photo-fragmentation[2,3] and Coulombic fission[4], producing atom and ion fragments with a few electronvolts (eV) of energy. However, recent studies of the photoionization of atomic cluster) are ionized, electrons undergo rapid collisional heating for the short time (<1 ps) before the cluster disassembles in the laser field[19]. Through various collective and nonlinear processes, the laser rapidly heats the electrons to a non-equilibrium state (with mean

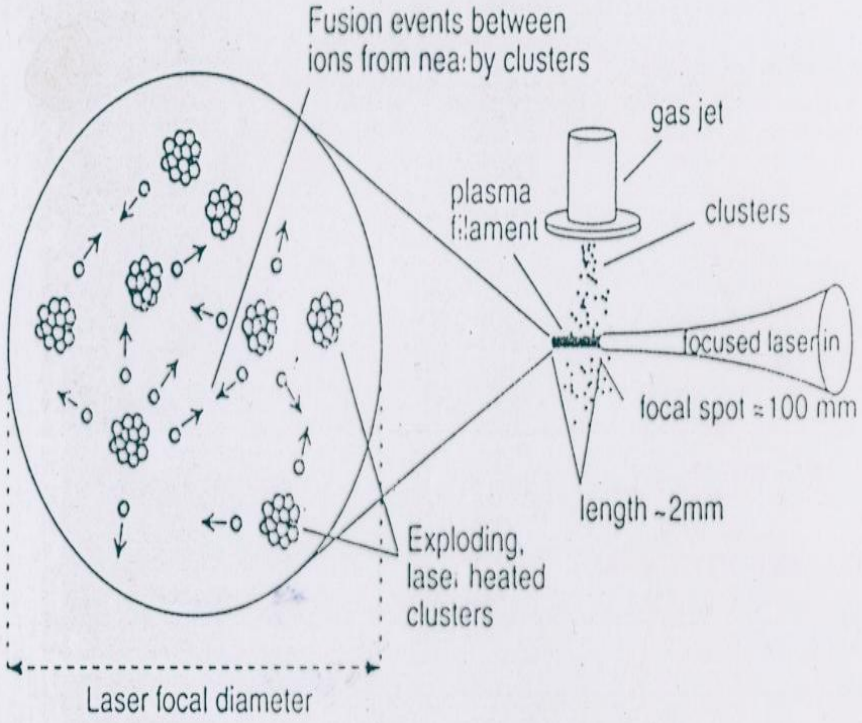

Figure 1 Layout of the deuterium cluster fusion experiment.

CREI~ Rc ~ 4 – 5 Å

Circular polarization Excitation at 800 nm I=10**14 W/cm2

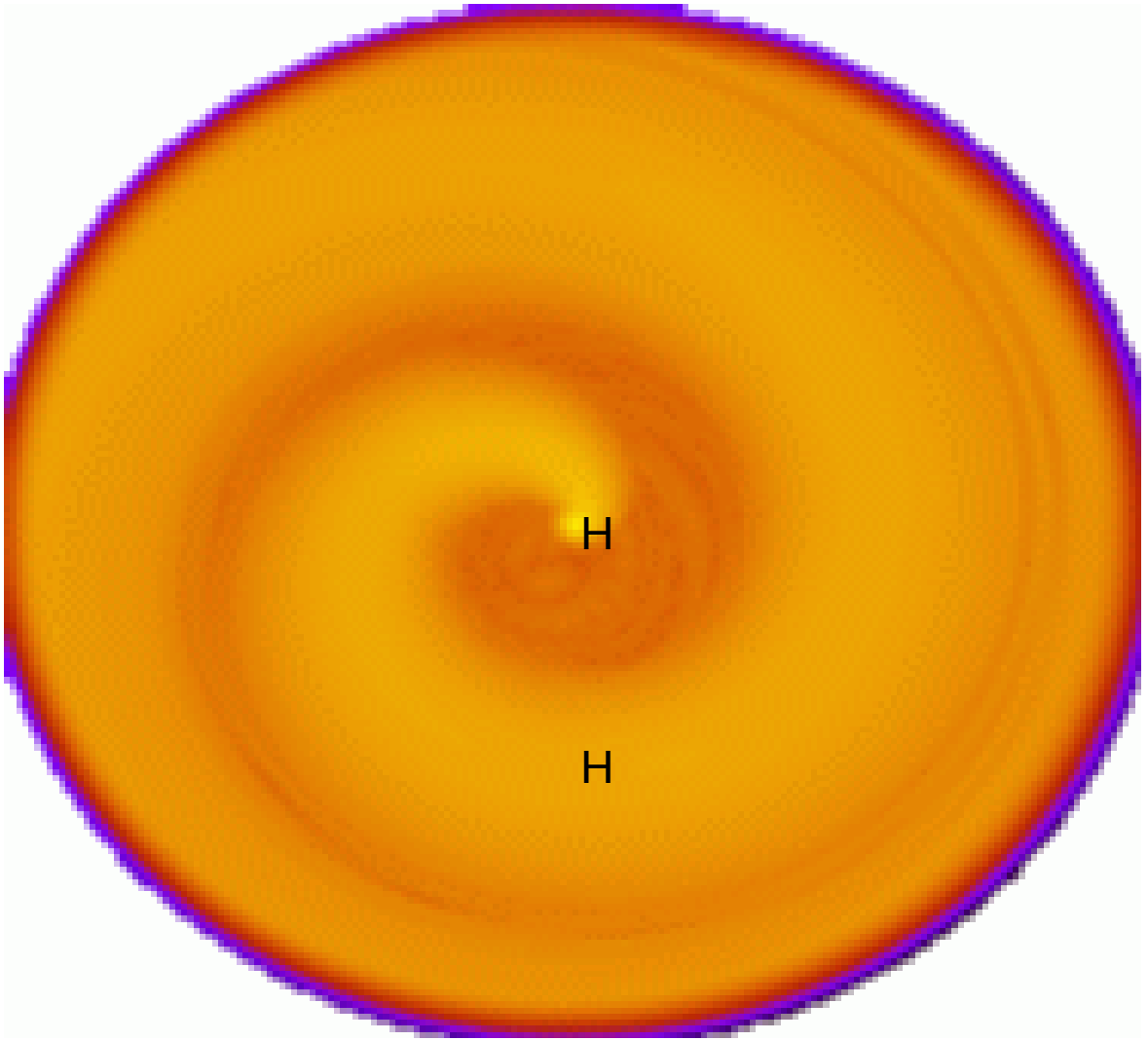

Electron Whirlpool – Tourbillon Electronique –
Elektronischer Wirbel (J Manz- FU Berlin)

Les lasers traquent les mouvements des électrons

>>> *Science* en juin, par une équipe internationale conduite par Martin Schultze, de l'université Ludwig Maximilians et du Max Planck Institut d'optique quantique, à Garching. Ils ont observé, pour la première fois, un délai entre les différents processus d'émissions de lumière provoqués par l'excitation d'un atome de néon. Un délai de 21 attosecondes, mesuré à 5 attosecondes près [8]. *« On observe là un phénomène que personne ne peut encore expliquer,* insiste Anne L'Huillier, *c'est vraiment de la nouvelle physique. »*

Manipulation à volonté. Tout aussi enthousiaste, Eleftherios Goulielmakis décrit déjà les prochaines étapes : *« Après les premières études sur des atomes simples, la physique attoseconde se tourne vers l'étude de molécules de plus en plus complexes, de plus en plus grosses. Progressivement, les efforts se porteront sur les macromolécules, par exemple les peptides pour la biochimie, ou les molécules mises en jeu dans le processus de la photosynthèse, et enfin pour progresser en physique des solides. »*

Pour le physicien, l'étape suivante sera alors de manipuler les électrons à l'aide des impulsions attosecondes : *« Nous travaillons à mettre au point une boîte à outils en ce sens, par exemple en sculptant la forme des impulsions pour agir sur les électrons. »* De quoi placer la physique attoseconde sur la voie dessinée, depuis les années 1980, par la microscopie à effet tunnel et à force atomique*. D'instruments imaginés au départ pour épier la matière ces microscopes ont fini par devenir de véritables couteaux suisses, permettant de manipuler atomes et molécules à volonté, à l'échelle du nanomètre. Les impulsions attosecondes en feront-elles autant avec des électrons, permettant par exemple de contrôler l'efficacité de certaines réactions chimiques, comme la photosynthèse ? *« Nous verrons les premiers résultats d'outils attosecondes dès l'an prochain »*, pronostique Eleftherios Goulielmakis.

Attophysique. À quand aussi une « attoélectronique » capable de redonner un coup de fouet à la physique des semi-conducteurs qui s'approche de ses limites ? Pour Anne L'Huillier, on en est encore loin : *« Tout le monde y pense bien évidemment mais rien n'est encore fait. Comme nous défrichons un domaine complètement vierge, de nouvelles questions surgissent à chaque résultat expérimental. C'est pour cette raison que le délai entre les expériences et les publications est très long. Il nous faut le temps de comprendre ce qu'on observe. »* De longs mois d'interprétation qui n'empêchent pas la véritable moisson de publications constatée cette année, et qui augurent déjà une année 2011 au moins aussi riche. Et notamment en Europe, puisque les réseaux de coopération scientifique sur la physique attoseconde qui s'y succèdent depuis 1992 – le dernier en date, Attofel, vient de démarrer – ont permis au Vieux Continent de prendre la tête de la compétition internationale pour la maîtrise de cette nouvelle physique. ■

* **LE MICROSCOPE À EFFET TUNNEL** utilise un phénomène quantique, l'effet tunnel, pour déterminer la topologie de surfaces avec une résolution voisine du nanomètre. Le microscope à force atomique en est un dérivé.

Une moisson de prix

Signe du fort dynamisme de la discipline, la physique attoseconde a eu les honneurs de trois prix prestigieux l'automne dernier. Anne L'Huillier (photo), de l'université de Lund, en Suède, est l'une des cinq lauréates du prix 2011 « Pour les femmes et la science » remis par l'Unesco et la fondation L'Oréal. Le jury était présidé cette année par le Prix Nobel Ahmed Zewail, couronné en 1999 pour ses travaux en physique femtoseconde. Début novembre, André Bandrauk, de l'université de Sherbrooke, au Canada, a reçu le prix Marie-Victorin, l'un des onze Prix du Québec remis chaque année par le gouvernement de la province canadienne. André Bandrauk est un théoricien qui a notamment travaillé sur le comportement des molécules dans des champs électromagnétiques intenses et la génération d'harmoniques. Enfin, mi-novembre, l'Autrichien Reihnard Kienberger s'est vu remettre le prix annuel de la Commission internationale pour l'optique (ICO). Il travaille en particulier sur la mesure des impulsions attosecondes uniques, au Max Planck Institut d'optique quantique, à Garching, en Allemagne. Tout comme Eleftherios Goulielmakis, récompensé cette année par le Prix du jeune chercheur de l'ICO. Si tout le monde se refuse à l'évoquer, l'idée qu'un Nobel puisse récompenser un jour l'« attophysique » est présente dans toutes les têtes.

© MONIQUE RUIZ/UNIVERSITÉ LAVAL (QUÉBEC) POUR LA FONDATION L'ORÉAL

[1] Pascal Salières, Thierry Ruchon et Bertrand Carré, « Des flashs toujours plus courts », *Les Dossiers de la Recherche*, p. 60, février 2010 ; Timothée Jamin, « Filmer le mouvement des électrons », *La Recherche*, novembre 2010, p. 68.
[2] D. H. Ko *et al.*, *New J. Phys.*, doi : 12063008, 2010.
[3] S. Haessler *et al.*, *Nature Physics*, 6, 200, 2010.
[4] E. Goulielmakis *et al.*, *Nature*, 466, 739, 2010.
[5] G. Sansone *et al.*, *Nature*, 465, 763, 2010.
[6] Y. Mairesse *et al.*, *Phys. Rev. Lett.*, 104, doi : 213601, 2010.
[7] H. Wörner *et al.*, *Nature*, 466, 604, 2010.
[8] M. Schultze *et al.*, *Science*, 328, 1658, 2010.

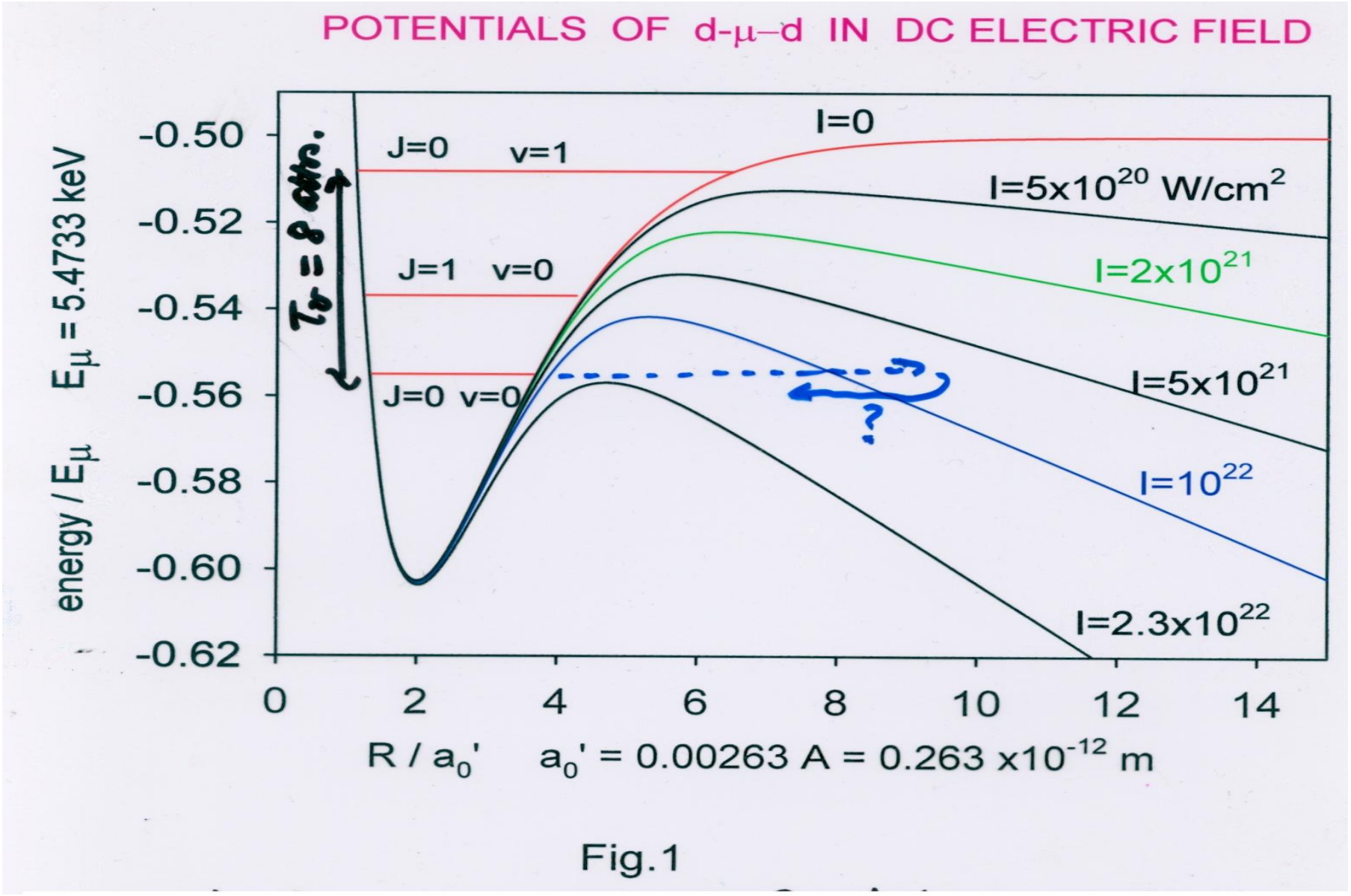

Fig.1

H^+_2 (Bond Softening / PH. Bucksbaum PR '90-92

A_{R2}^+ (Bond Softening / ADB (JCP 1981)

Classement Top 500 des supercalculateurs

L'ordinateur le plus puissant au Canada à l'Université de Sherbrooke

Mammouth, l'ordinateur le plus puissant au Canada selon le dernier classement international Top 500 des supercalculateurs

Photo : Alain Veilleux

14 novembre 2011
Nouvelles UdeS

Selon le dernier classement international Top 500 des supercalculateurs, l'Université héberge le plus puissant outil de calcul scientifique au Canada, et le 41e plus puissant au monde. Nommé «Mammouth» et possédant la mémoire et la vitesse combinées d'environ 20 000 ordinateurs personnels de dernière génération, ce superordinateur effectue des calculs d'une ampleur jusqu'ici inégalée au pays.

Grâce à Mammouth, des équipes provenant de plusieurs universités du Québec et du Canada peuvent réaliser des simulations numériques essentielles à leurs recherches dans différents secteurs du génie, des sciences, de la médecine et même dans des secteurs traditionnellement moins associés au calcul scientifique, comme l'économie et la linguistique.

Mammouth consiste en 1630 serveurs comportant un total de 39 648 processeurs (cœurs) AMD, une mémoire vive totale de 57 600 giga-octets et une capacité de stockage de données de 500 000 giga-octets. Il peut effectuer 240 000 milliards d'opérations arithmétiques par seconde.

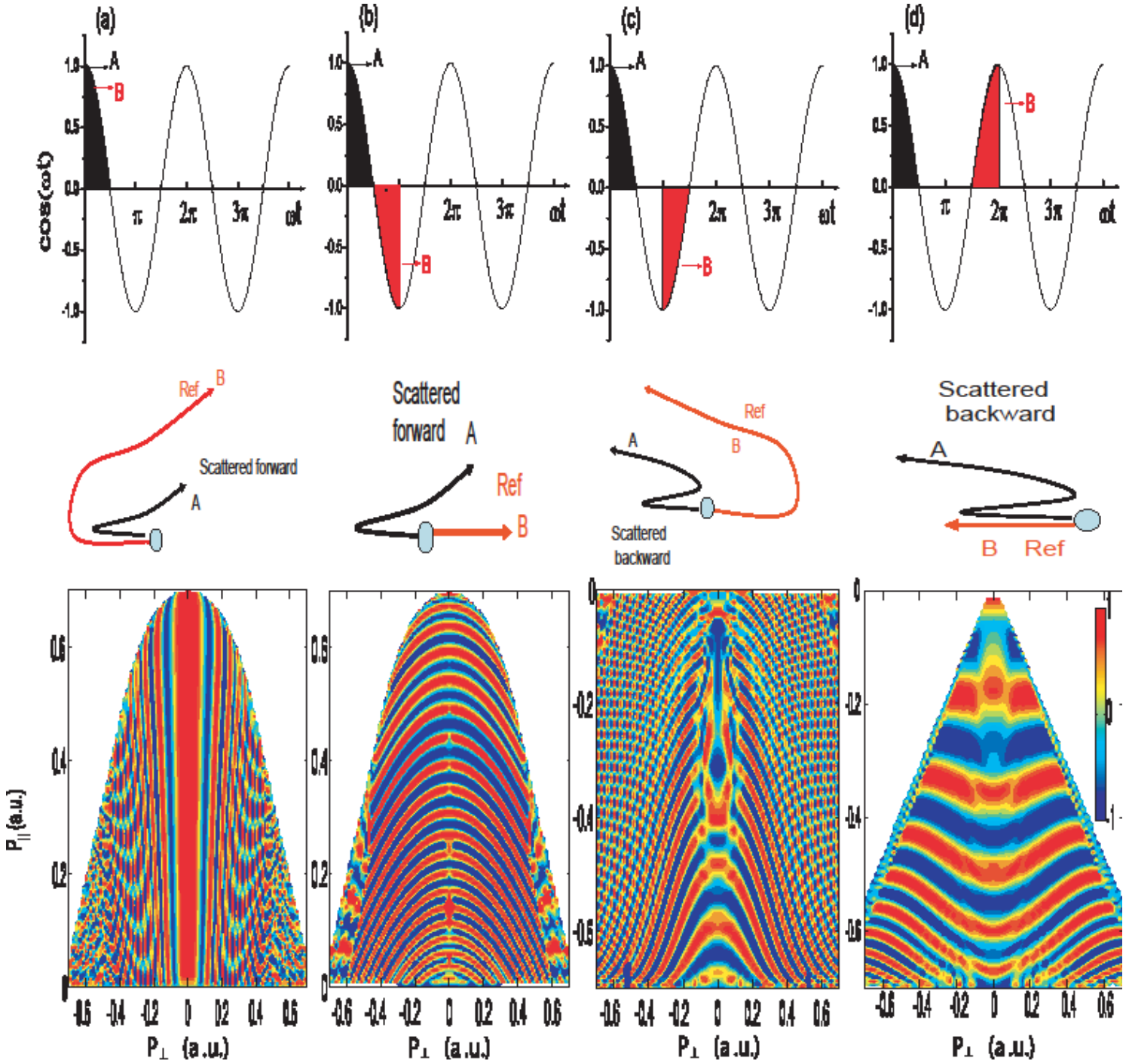
(a)
(b)
(c)
(d)
A
B
cos(ωt)
π
2π
3π
ωt
Ref
Scattered forward
Scattered backward
P|| (a.u.)
P⊥ (a.u.)

$$a_W(\omega,t)=\sqrt{\frac{\omega}{\pi^{1/2}\sigma}}\int_{-\infty}^{\infty}\exp(-i\omega t')\exp[-\frac{\omega^2(t'-t)^2}{2\sigma^2}]a(t')dt'$$

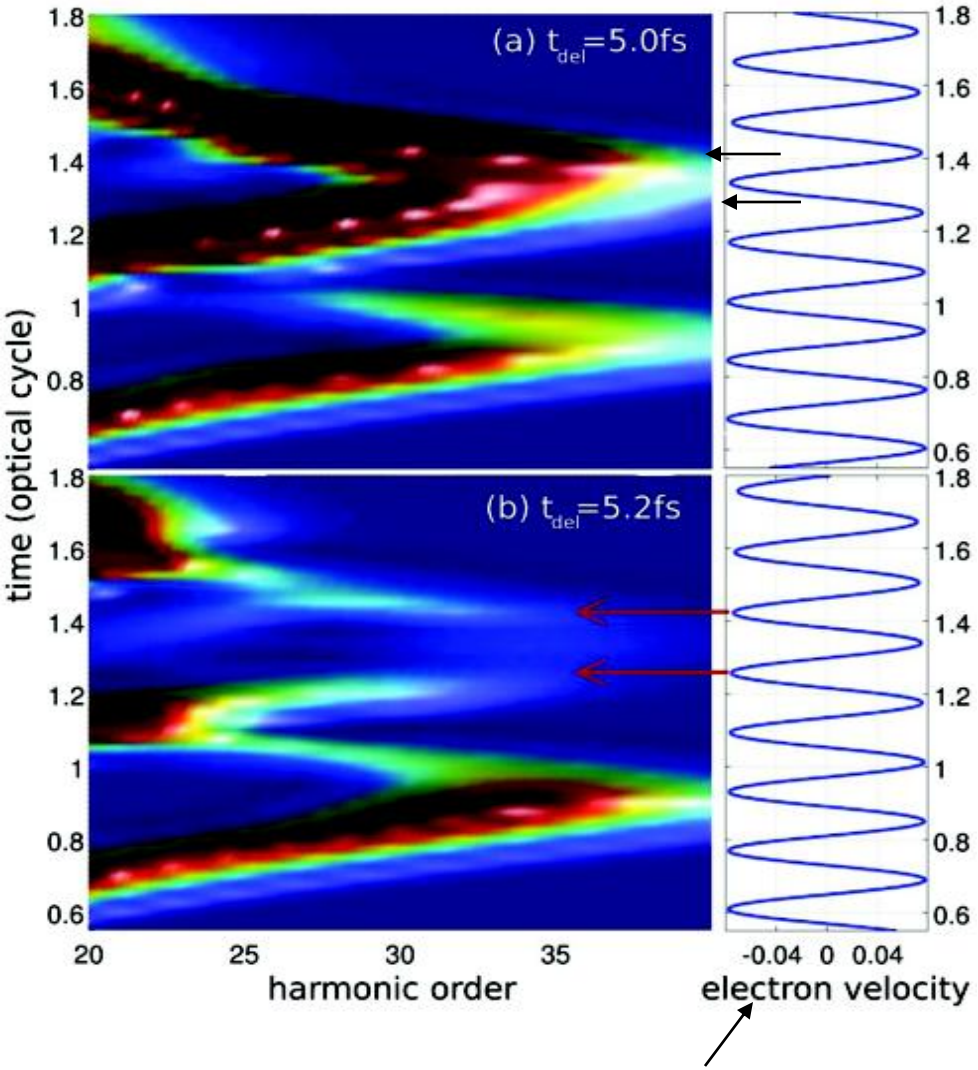

H.Niikura,D. Villeneuve, P.B. Corkum, PRL 94, 083003 (2005)

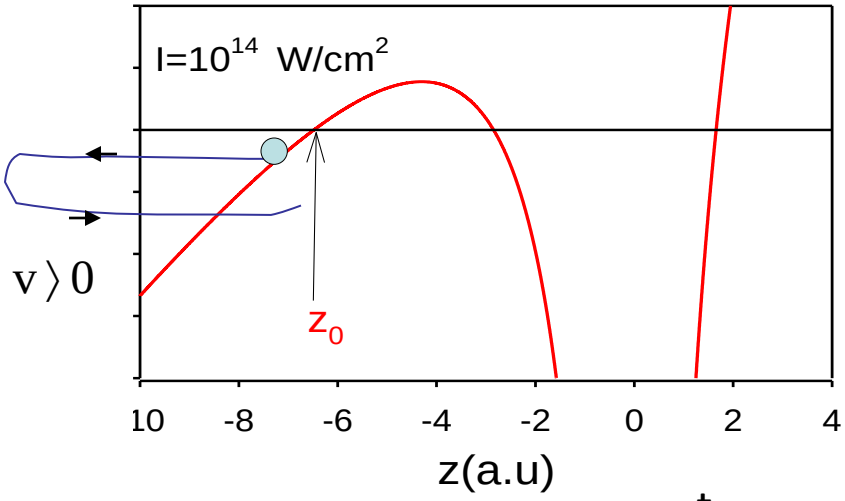

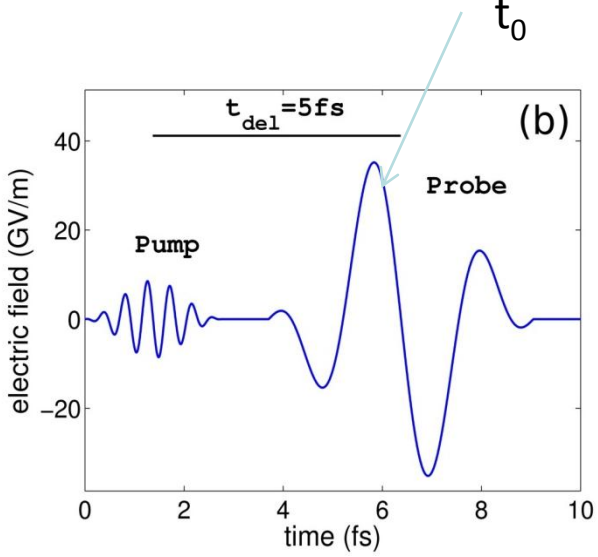

Vitesse moyenne de l'électron sans l'impulsion sonde